

Chapter 2

Vision's First Steps: Anatomy, Physiology, and Perception in the Retina, Lateral Geniculate Nucleus, and Early Visual Cortical Areas

Xoana G. Troncoso, Stephen L. Macknik, and Susana Martinez-Conde

Abstract This chapter reviews the functional anatomical bases of visual perception in the retina, the lateral geniculate nucleus (LGN) in the visual thalamus, the primary visual cortex (area V1, also called the striate cortex, and Brodmann area 17), and the extrastriate visual cortical areas of the dorsal and ventral pathways.

The sections dedicated to the retina and LGN review the basic anatomical and laminar organization of these two areas, as well as their retinotopic organization and receptive field structure. We also describe the anatomical and functional differences among the magnocellular, parvocellular and koniocellular pathways.

The section dedicated to area V1 reviews the functional maps in this area (retinotopic map, ocular dominance map, orientation selectivity map), as well as their anatomical relationship to each other. Special attention is given to the modular columnar organization of area V1, and to the various receptive field classes in V1 neurons.

The section dedicated to extrastriate cortical visual areas describes the “where” and “what” pathways in the dorsal and ventral visual streams, and their respective physiological functions.

The temporal dynamics of neurons throughout the visual pathway are critical to understanding visibility and neural information processing. We discuss the role of lateral inhibition circuits in processing spatiotemporal edges, corners, and in the temporal dynamics of vision.

We also discuss the effects of eye movements on visual physiology and perception in early visual areas. Our visual and oculomotor systems must achieve a very delicate balance: insufficient eye movements lead to adaptation and visual fading, whereas excessive motion of the eyes produces blurring and unstable vision during fixation. These issues are very important for neural prosthetics, in which electrodes are stabilized on the substrate.

S. Martinez-Conde (✉)

Barrow Neurological Institute, 350 W. Thomas Road, Phoenix, AZ 85013, USA

e-mail: smart@neuralcorrelate.com

Finally, another critical issue for neural prosthetics concerns the neural code for visual perception: How can the electrical activity of a neuron, or a neuronal population, encode and transmit visual information about an object? Here we will discuss how neurons of early visual areas may communicate information about the visible world to each other.

Abbreviations

area MST	Medial superior temporal area
area MT	Middle temporal visual area
area V1	Primary visual cortex
DOG	Difference of gaussians
GABA	Gamma-aminobutyric acid
LGN	Lateral geniculate nucleus

2.1 Introduction

The process of “seeing” is complex and not well understood. But we do know that individual neurons in the early visual system are tuned to stimuli with specific attributes (such as color, shape, brightness, position on the retina, etc.). The receptive field of a visual neuron is the area of the visual field (or its corresponding region on the retina) that when stimulated (by light or electrical impulses) can influence the response of the neuron (Fig. 2.1). Visual stimuli outside a neuron’s receptive field



Fig. 2.1 Activation of retinal photoreceptors and their corresponding receptive fields during visual exploration. The eye focuses light that is reflected from the visual image onto the retina, upside down and backwards. Adjacent photoreceptors within the retina are activated by adjacent points of light from the painting. Figure by the Barrow Neurological Institute Illustrations Department

produce no effect on the neuron's responses. Understanding the precise receptive field structure of a given neuron is crucial to understanding and predicting its responses to specific stimuli. For instance, some early receptive fields have a spatial substructure (while others do not), and stimulating their different subregions results in increases or decreases in neural activity. A visual neural prosthesis should ultimately replace the visual processing represented by the receptive fields at a given (damaged or otherwise impaired) stage of the visual hierarchy. A close replication of the output of the replaced neurons will ensure that the healthy tissue farther along the visual pathway receives properly structured inputs.

2.2 Retina

2.2.1 Anatomy

Vision starts in the retina: it is here where photons are converted into electrical signals, to be then interpreted by the brain to construct our perception of the visual world.

The retina has the shape of a bowl (about 0.4 mm thick in adult humans). It is a well organized structure with three main layers (called the nuclear layers) of neuronal bodies. These main layers are separated by two other layers containing synapses made by axons and dendrites (called the plexiform layers). The basic retinal cell classes and their interconnections were revealed by Ramón y Cajal over a century ago [175] (Fig. 2.2).

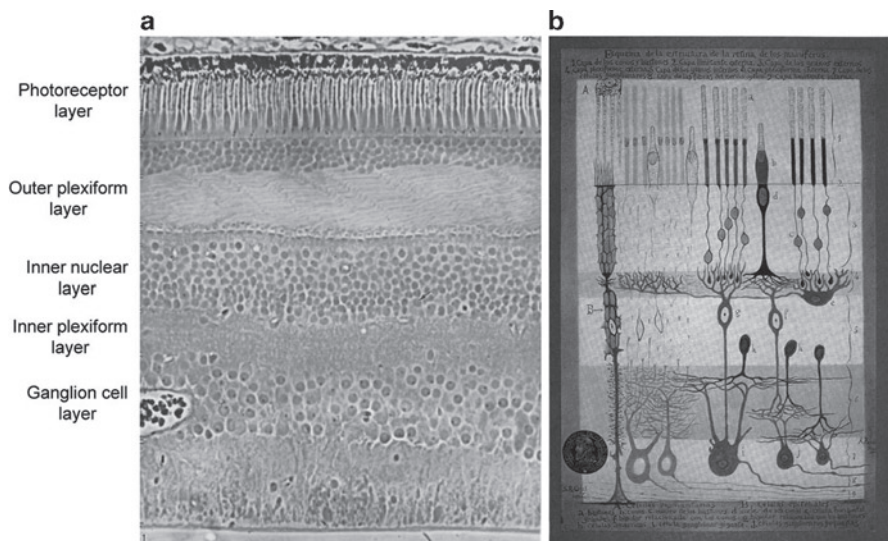


Fig. 2.2 Retinal layers. (a) Light micrograph of a vertical section of the human retina from [29]. (b) Cross-sectional microscopic drawing by Ramón y Cajal from [127, 176]

The functional anatomy of the retina is enormously rich and complicated. A short overview is provided here, to set a basis to understand the next few stages of the visual hierarchy.

The three nuclear layers are the photoreceptor layer (which lies on the back on the retina, farthest from the light coming in), the inner nuclear cell layer (in the middle) and the ganglion cell layer (nearest to the center of the eye).

Photoreceptor layer: light is transduced into electrical signals by photoreceptors: rods and cones. Cones are not sensitive to dim light, but under photopic conditions (bright light) they are responsible for fine detail and color vision. Rods are responsible for our vision under scotopic conditions (dim light), and saturate when the level of light is high. Rods and cones are distributed across the retina with very different profiles: in the fovea, where our fine vision is most detailed, cones are very densely packed (up to 160,000 cones/mm²) but cone density drops rapidly as we move away from the fovea. Rods are absent from the fovea [190], but their density rises quickly to reach a peak at an eccentricity between 5 and 7 mm, beyond which they steadily decline in number [45, 46, 164]. Humans have one type of rod and three types of cones. The three types of cones, responsible for color vision, are called L (or red) cones, M (or green) cones, and S (or blue) cones, and they are most sensitive to different segments of the spectrum of light: L cones are most sensitive to long wavelengths (peak sensitivity at 564 nm), M cones are most sensitive to middle wavelengths (peak sensitivity at 533 nm) and S cones are most sensitive to short wavelengths (peak sensitivity at 437 nm) [32, 33, 131]. L, M, and S cones are distributed in the retina in a particular way: only 10% of the cones are S cones, and they are absent from the fovea. Although L cones and M cones are randomly intermixed, there are ~2 times more L cones than M cones [1, 41, 44, 152, 187].

Inner nuclear layer: contains three classes of neurons: horizontal cells, bipolar cells, and amacrine cells. Horizontal cells have their bodies in the inner nuclear layer and connect to photoreceptors (through chemical synapses) and other horizontal cells (through gap junctions) in the outer plexiform layer [223]. Horizontal cells receive input from photoreceptors, but they also give output to the same photoreceptors, providing lateral inhibition, which acts to enhance spatial differences in photoreceptor activation at the level of the bipolar cells [49, 222]. There are over 13 different types of bipolar cells [30, 105] and all of them have some dendritic processes in the outer plexiform layer, the soma in the inner nuclear layer and some axon terminals in the inner plexiform layer [66]. The dendritic processes of a bipolar cell receive input from one type of photoreceptor (either from cones or from rods, but never from both) [186]. Each bipolar cell then conveys its response to the inner plexiform layer, where it contacts both amacrine and ganglion cells [49]. Amacrine cells (over 30 different types), receive input from bipolar cells and other amacrine cells, and pass their messages onto bipolar cells, other amacrine cells, and ganglion cells [50, 128]. Different types of amacrine cells may have different functions in retinal processing, but their specific roles remain unknown for the most part.

Ganglion cell layer: there are more than 20 different ganglion cell types [105], and many of them are specialized on coding some particular aspect of the visual world such as sign-of-contrast and color [186]. Ganglion cells receive their input from

amacrine and bipolar cells, and send their outputs to the brain in the form of action potentials through the optic nerve. These are the first cells in the visual pathway that produce action potentials (all-or-none) as their output; all the previous cell classes (photoreceptors, horizontal, bipolar and amacrine cells) release their neurotransmitters in response to graded potentials. Even though there are over 20 different types of ganglion cells, two of them account for almost 80% of the ganglion cell population [171]: the midget and the parasol ganglion cells, named by Polyak [173]. Near the fovea each midget ganglion cell receives direct input from only one midget bipolar cell [104, 106] and thus has a very small and compact receptive field (it collects input from a small number of cones). Parasol cells receive their direct input from diffuse bipolar cells, have larger dendritic fields, and thus receive input from many more cones [224]. The dendritic field size increases with eccentricity for both types of cells [48, 51, 224]. Away from the fovea, the increase in dendritic field size with retinal eccentricity is more or less matched by a decrease in spatial density, so the amount of retina covered is approximately constant over most of the retina [224].

2.2.2 Physiology and Receptive Fields

The receptive fields of ganglion cells in the retina are approximately circular and have functionally distinct central and peripheral regions (called center and surround); stimulation of these two regions produces opposite and antagonistic effects upon the activity of the ganglion cells. Ganglion cells respond optimally to differential illumination of the receptive field center and surround. Diffuse illumination of the whole receptive field produces only weak responses. There are two main types of center-surround receptive fields: on-center receptive fields respond best to light falling on the center, and darkness falling on the surround; off-center receptive fields respond best to darkness on the center and light on the surround (Fig. 2.3). The properties of center-surround receptive fields change during scotopic conditions: the size of the receptive field center usually increases, the surround strength diminishes and there is a longer latency for the response [16, 28, 65, 144, 156, 167].

Werblin and Dowling [225], and Kaneko [99] discovered that bipolar cells also have center-surround receptive fields.

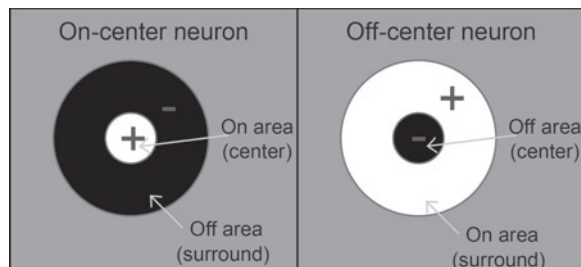


Fig. 2.3 Concentric receptive fields of retinal ganglion neurons

In the dark, photoreceptors are depolarized and continuously active [205], releasing glutamate to bipolar and horizontal cells. When light arrives and the photo pigments bleach within a photoreceptor, that photoreceptor hyperpolarizes, and the amount of glutamate released decreases in a graded manner, as a function of the number of photons [204]. All photoreceptors use the same neurotransmitter, glutamate, and so on-center and off-center bipolar cells acquire their preference by having one of two types of glutamate receptor [150]:

- On-center bipolar cells have metabotropic receptors that make the cell hyperpolarize when they receive glutamate [159, 199]. When light hits photoreceptors, they hyperpolarize and release less glutamate. This reduces the inhibition in the bipolar cells that therefore increase their activity. In the dark, photoreceptors depolarize and release more glutamate. Therefore the bipolar cells hyperpolarize.
- Off-center bipolar cells have ionotropic receptors that depolarize the cell when receiving glutamate [161, 200]. In this case, when light arrives to the retina, the photoreceptors hyperpolarize and release less glutamate. Consequently, the bipolar cells decrease their activity. In the dark, the photoreceptors depolarize and release more glutamate. As a consequence, the bipolar cells depolarize.

Both on- and off-bipolar cells make the same kind of contacts in the inner plexiform layer. All bipolar cells release glutamate as their neurotransmitter and all the ganglion cells have ionotropic receptors: therefore, ganglion cells that receive input from on-center bipolar cells are also on-center. Ganglion cells that receive input from off-center bipolar cells are off-center [186]. In 1978 Nelson et al. discovered that there is a clear anatomical difference between on- and off-bipolar cells: they synapse onto ganglion and amacrine cells within different sublayers within the inner plexiform layer. The off-center bipolar dendrites make synapses closer to the inner nuclear layer whereas the on-center bipolar dendrites terminate closer to the ganglion cell layer [47, 160].

As described earlier, there are two predominant types of ganglion cells: midget and parasol [173]. Both types of ganglion cells have center-surround receptive fields with similar spatial organization, but physiological studies have described several differences between them: parasol cells respond more transiently to light onset or offset than midget cells [82]; parasol cells have larger receptive fields centers than midget cells at the same eccentricity [55]; most midget cells have spectral selectivity and antagonism while most parasol cells do not [55, 57, 82]; parasol cells respond much more vigorously than midget cells to small changes in luminance contrast [102]. The anatomical and functional differences between midget and parasol cells lead to two different visual pathways that remain segregated throughout the early visual system. The parvocellular pathway starts with the midget cells and is very sensitive to color and spatial frequency. The magnocellular pathway starts with the parasol cells and is most sensitive to luminance contrast and temporal frequency.

Due to the center-surround organization of the ganglion cell receptive fields, these neurons are quite insensitive to changes in overall levels of luminance. They signal differences within their receptive fields by comparing the degree of illumination between the center and the surround.

2.3 LGN

All retinal ganglion cells send their axons to the brain via the optic nerve. The axons decussate at the optic chiasm, so the information from each nasal hemiretina is sent to the contralateral hemisphere. Retinal ganglion cells project to three major subcortical targets: the pretectum, the superior colliculus, and the lateral geniculate nucleus (LGN) of the thalamus. The LGN is the principal structure that sends visual information to the visual cortex, with input from 90% of the retinal ganglion cells. The LGN is laid out so that neighboring neurons are stimulated by adjacent regions in visual space. This property is called retinotopic organization.

In primates, the LGN contains six layers of cell bodies that can be classified in two groups according to their histological characteristics: the two bottom layers (ventral) contain large cell bodies and are called magnocellular layers; cells in the four upper layers (dorsal) are smaller and are called the parvocellular layers. The parvocellular layers receive their main inputs from the midget ganglion cells in the retina. The magnocellular layers receive their main inputs from parasol ganglion cells [42, 109, 170, 189, 192]. Between each of the magno and parvo layers lies a zone of very small cells: the koniocellular layers. Konio cells are functionally and neurochemically distinct from magno and parvo cells [87]. The finest caliber retinal axons, presumably originating from retinal ganglion cells that are morphologically distinct from those projecting to magno and parvo layers [109], innervate the koniocellular layers [42]. The koniocellular pathway starts with the small bistratified ganglion cells of the retina that are sensitive to blue (or S-cone) activation. The koniocellular layers interdigitate between the primary six layers of the LGN [86].

Each LGN receives input from both eyes, but the input from each eye is segregated to different monocular layers: layers 1, 3, and 6 get input from the contralateral eye, whereas layers 2, 4, and 5 get input from the ipsilateral eye [94].

Hubel and Wiesel discovered that LGN receptive fields have a similar center-surround configuration to retinal ganglion cells, however the suppressive strength of the surround is stronger than in retinal cells [90].

Virtually all parvocellular cells (99%) present linear spatial summation. That is, the response to two elements presented simultaneously to the receptive field equals the sum of the response to each of the elements presented separately. About 75% of magnocellular cells are also linear, the other 25% are not [101].

The LGN is often called a relay nucleus because it is the only structure between the retina and the cortex. However, LGN neurons are part of a complex circuit that involves ascending, descending and recurrent sets of neuronal connections [5, 194, 201]. The major source of descending input comes from neurons in layer 6 of V1. These feedback connections can be excitatory (through direct monosynaptic connections) or inhibitory (through inhibitory interneurons in the LGN or the reticular nucleus of the thalamus) [67, 83]. The functions of the corticothalamic pathway are still under discussion [5]. These connections

could help to explain LGN neurons' extra-classical receptive field properties, such as the effects of suppressive field [5, 27, 38, 158]. It is generally agreed that these feedback connections act by modulating the responsiveness of the LGN neurons, and not by driving the actual responses [193]. It is possible that the major role of feedback in the visual system is to maintain top-down attention [124, 125].

2.4 V1

2.4.1 *Anatomy*

LGN neurons send their axons through the optic radiations to the back of the brain, where the primary visual cortex, area V1, is located. V1 is virtually the only target of primate LGN neurons [19, 35]. The magnocellular and parvocellular pathways that started in the retina remain largely separated.

V1, like most cortical areas, has six main layers [31]. Most of the LGN inputs arrive to layer 4, which is divided in four sublayers: sublayer 4C α receives axons mostly from magnocellular neurons. Sublayer 4C β (and sublayer 4A to a lesser extent) receives axons mostly from parvocellular neurons. Layer 6 receives weak input from collaterals of the same LGN axons that provide strong input to layer 4C [22, 85, 94, 116]. Neurons from the koniocellular layers in the LGN send their axons to layer 1 and layers 2–3 [87, 112].

Layer 4C α sends its output to 4B [37, 72, 117]. Axons from neurons in 4C β terminate in the deepest part of layer 3 [37, 72, 107]. Layers 2, 3, and 4B project mainly to other cortical regions [36] and also send axons to layer 5 [23]. Layer 5 projects back to layers 4B, 2, 3 [37] and to the superior colliculus [118]. Layer 6 projects to the LGN [73, 227] and also sends axons to several V1 layers [117, 227]. Many of the projection pyramidal cells in layers 2, 3, 4B, 5 and 6 have collaterals that connect locally. Layer 1 contains few cell bodies, but many axons and dendrites synapse there [119]. Figure 2.4 shows a schematic representation of the main connections.

In addition to the feedforward input coming from the LGN, V1 receives direct feedback from areas V2, V3, V4, V5 (or MT), MST, FEF, LIP and inferotemporal cortex [17, 169, 184, 196, 203, 213, 214]. The projections from these areas terminate in layers 1, 2, and 5 of V1, with occasional arbors in layer 3 [185, 197].

2.4.2 *Physiology and Receptive Fields*

In primates, the receptive fields of most V1 input neurons (layer 4C) have the same center-surround organization as the LGN neurons they receive direct input from [18, 21, 34, 113, 172]. Outside of layer 4C, the receptive field structure is very

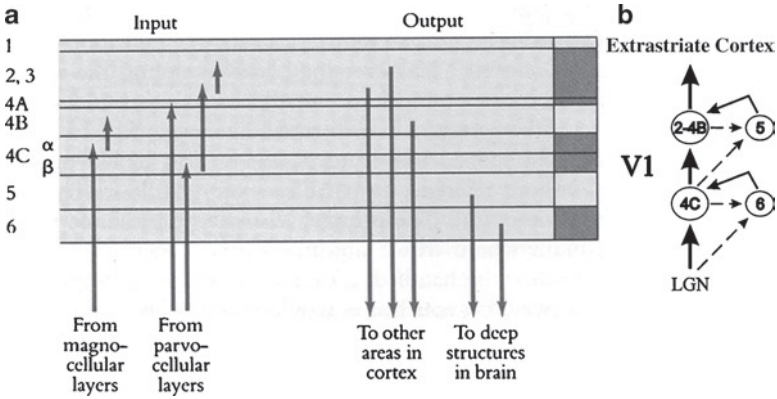


Fig. 2.4 Schematic representation of V1 inputs, outputs and vertical interconnections. (a) From [88]. (b) From [36]

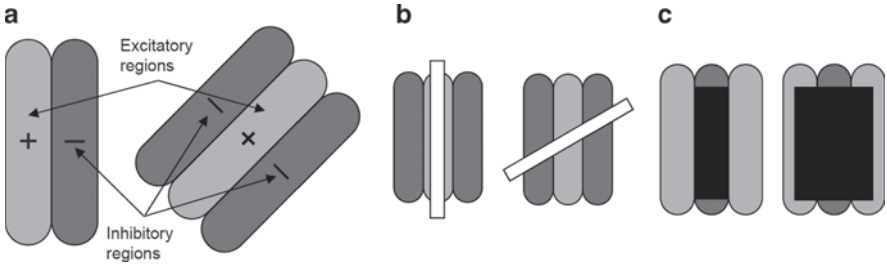


Fig. 2.5 (a) Schematic representation of simple cell receptive fields with different orientations and number of subregions. (b) Receptive field selective to vertical orientations. A vertical light bar over the excitatory region is the optimal stimulus (left). A non-vertical light bar (right) that partially falls on the inhibitory regions makes the cell fire less. (c) Cell stimulated with a bar of the preferred spatial frequency (left) and with a bar that is too wide and thus falls on the opposite contrast subregions

different and we can distinguish two main groups of cells according to their receptive field type: simple cells and complex cells [91].

Simple cells: Hubel and Wiesel first described the receptive fields of “simple cells” in area V1 [89]. The receptive fields of simple cells are organized in distinct elongated on and off antagonistic subregions, whose spatial arrangement determines the responses of the neuron to different stimuli. Simple cells are selective to the orientation and spatial frequency of the stimulus (Fig. 2.5). The response of simple neurons is reduced when there is a mismatch between the light and dark parts of the stimulus and the on- and off-regions of the receptive field. By testing the neuron’s responses to different stimuli, it is possible to generate tuning curves for orientation and spatial frequency.

Hubel and Wiesel [91] proposed that each simple cell gets its input from an array of center-surround receptive fields of the same sign that have their centers arranged

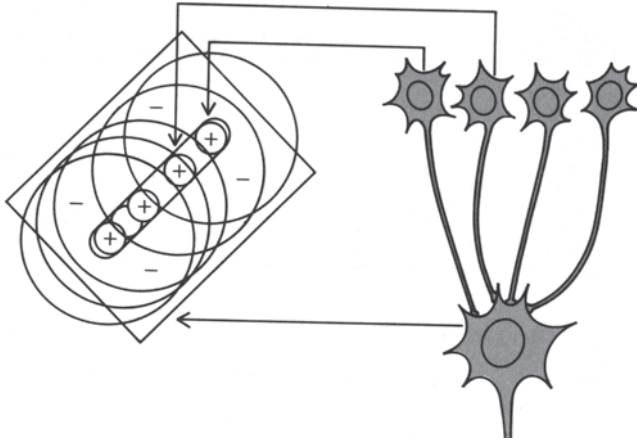
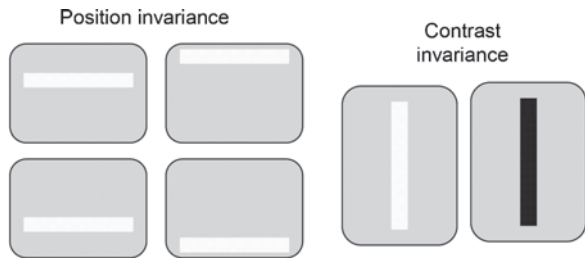


Fig. 2.6 Schematic representation of the feed forward excitatory model proposed by Hubel and Wiesel in 1962. From [91]

Fig. 2.7 A complex cell gives the same response to bars anywhere within the receptive field, and does not prefer either light or dark bars



along a straight line on the retina. The synapses from the center-surround receptive fields to the simple cell are excitatory and this gives the simple receptive fields its elongated shape and orientation selectivity (Fig. 2.6). Recent studies have provided strong support for this model [9, 69–71, 180, 216].

Complex cells: complex cells in the primary visual cortex, discovered by Hubel and Wiesel, are selective to the orientation and spatial frequency of stimuli (like simple cells) but their receptive fields do not have distinctive on and off subregions [91]. Consequently, complex receptive fields are invariant to the spatial phase (position of the stimulus within the receptive field) and contrast polarity of the stimulus. When a single bar is presented within the receptive field, complex cells respond equally well regardless of the bar's position and contrast, as long as the bar has the preferred orientation and width (Fig. 2.7). When pairs of bars are presented simultaneously within the receptive field, complex cells exhibit nonlinearity in spatial summation [91]: the response to simultaneous presentation of two stimuli cannot be predicted from the sum of the responses to the two stimuli presented individually.

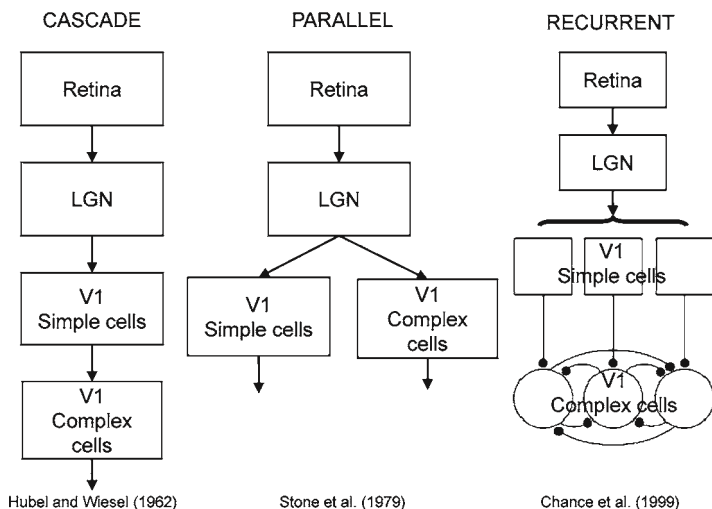


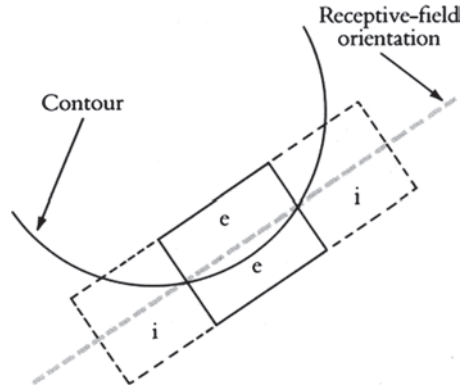
Fig. 2.8 Different hypothesis about the connectivity of complex cells. After [142]

This is a fundamental property of complex cells; simple cells are more or less linear [39, 91, 155, 182].

The circuits that give rise to complex cells is not fully understood; there are several different hypotheses in the literature, some of which are shown in Fig. 2.8. The “cascade model” [91] suggests that simple cells and complex cells represent two successive stages in hierarchical processing: in a first stage, simple cells are created from the convergence of center-surround inputs that have receptive fields aligned in visual space. In the second stage, complex cells are then generated by the convergence of simple cells inputs with similar orientation preferences (Fig. 2.8, left). “Parallel models” [202] propose that simple cells and complex cells are both constructed from direct geniculate inputs. Simple cells are created from the convergence of linear LGN inputs, and complex cells from the convergence of non-linear LGN inputs (Fig. 2.8, middle). “Recurrent models” [40] use a combination of weak simple cell inputs and strong recurrent complex cell inputs to generate complex cell nonlinearities (Fig. 2.8, right). Martinez and Alonso [8, 142, 143] published evidence supporting the Hubel and Wiesel cascade model.

End-stopped cells: ordinary simple and complex cells show length summation: the longer the bar stimulus, the better the response, until the bar is as long as the receptive field; making the bar even longer has no further effect. For end-stopped cells, lengthening the bar improves the response up to some limit, but exceeding that limit in one or both directions results in a weaker response. The same stimulus orientation evokes maximal excitation on the activating region and maximal inhibition on the outlying areas. Hubel and Wiesel discovered and characterized end-stopped cells in cat areas 18 and 19 and initially called them hypercomplex cells [92]. Later Gilbert showed that some simple and complex cells in cat area 17 are also end-stopped [25, 78]. Several recent studies suggest that most primate V1 cells

Fig. 2.9 A curved border would be a good stimulus for the end-stopped cell represented in the diagram. From [88]



are somewhat end-stopped [97, 100, 103, 165, 188]. The receptive field structure of end-stopped cells makes them especially sensitive to corners, curvature and terminators [88, 92] (Fig. 2.9).

Columnar organization: A fundamental feature of cortical organization is the spatial grouping of neurons with similar properties. V1 is functionally organized in layers and cortical columns, which are roughly perpendicular to the layers. The concept of cortical columns was introduced by Mountcastle in the somatosensory system [153, 154, 174], although Lorente de Nó had envisaged their existence through his anatomical studies [114]. Hubel and Wiesel discovered columnar organization in area V1, first in the cat [91] and then in the primate [93, 95, 226]. They showed that V1 cells with similar properties are grouped into columns: as they advanced an electrode in an orthogonal penetration from the cortex surface, they found that the neurons recorded by the electrode had similar receptive field axis orientation, ocular dominance, and position in the visual field.

- Ocular dominance columns: the inputs from the two eyes are segregated in layer 4, where cortical neurons are driven monocularly. In any given column extending above and below layer 4, all the cortical neurons, even if driven by both eyes, share the same eye preference. Ocular dominance columns form an interdigitating pattern on the cortex [91, 93, 226]. Figure 2.10 shows an ocular dominance map obtained with intrinsic optical imaging: we can see distinct strips in a 1 cm² patch of cortex, activated by a stationary bar presented monocularly to the visual system of a rhesus monkey.
- Orientation columns: Hubel and Wiesel [91, 93, 95] found that, just as with eye dominance, orientation preference remains constant in orthogonal penetrations through the cortical surface: the cortex is subdivided into narrow regions of constant orientation, extending from the surface to the white matter but interrupted by layer 4C, where most cells have no orientation preference [18, 21, 34, 113, 172] (although some recent studies have found orientation selective cells in layer 4C [84, 181, 191]). In a tangential electrode penetration, the orientation

Fig. 2.10 A 1 cm² image from cortical area V1 in a primate. The *stripes* indicate an ocular dominance map created when visual stimuli are displayed to the right eye versus the left eye [121]

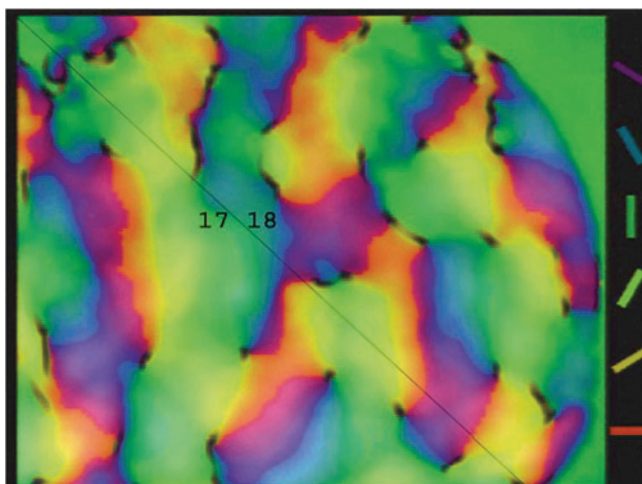
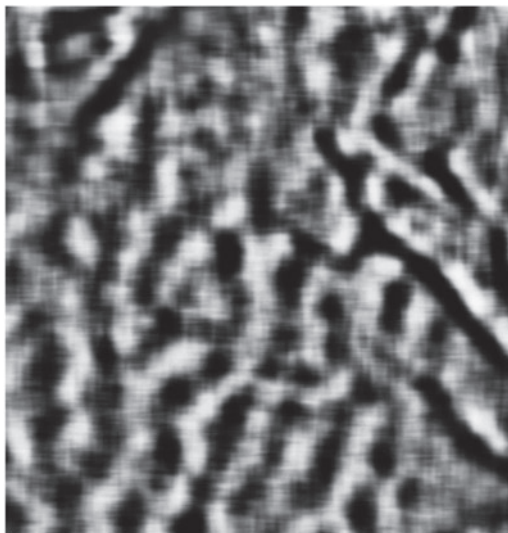


Fig. 2.11 An orientation map of the V1/V2 border from a cat (V1 and V2 are called area 17 and 18 in cats, by convention) obtained with intrinsic optical imaging. The legend on the right shows the relationship between the color of each pixel and orientation. The brightness of each pixel indicates the selectivity of each point in the map: *dark* indicates points in the map that are not particularly selective to any orientation, while *bright* points signify points in the map that are tuned specifically to a given orientation [127]

preference usually changes gradually. Figure 2.11 shows an orientation selectivity map in areas 17 and 18 of the cat visual cortex (equivalent to areas V1 and V2 in the primate) obtained with optical intrinsic signal: the image shows the preference of neurons to lines of different orientations, when presented to the retina.

Optical imaging studies have provided precise details about the columnar organization: orientation columns are arranged radially into pinwheel-like structures with orientation preference shifting gradually along contours circling the pinwheel center [20, 26]. Each pinwheel center tends to occur near the center of an ocular dominance patch [43, 115], and iso-orientation contours tend to cross ocular dominance boundaries at right angles [162]. Cortical columns where orientation preference changes smoothly or remains essentially constant are interspersed with regions containing orientation singularities where the orientation changes abruptly by up to 90° [24, 26, 54, 95, 211].

Horizontal and feedback connections: Many local connections in V1 have a wide lateral distribution, including long intralaminar connections spreading several millimeters [36]. Prominent horizontal connections are those originating from and terminating in layers 2–3 and 4B; these connections arise from neurons whose long-distance axon collaterals form periodic clusters [10, 37, 80, 81, 146, 183]. These clusters tend to preferentially link columns of neurons with similar response properties: in cats, ferrets, and monkeys they preferentially link columns with similar orientation preference [130, 212]. Feedback connections from extrastriate cortex to V1 also show an orderly topographic organization and terminate in a patch-like manner within V1 [11]. These two types of orderly connections (horizontal and feedback) may be involved in the generation of suppressive fields in V1 neurons, as well as other extra-classical receptive field modulations [11, 38, 39, 79, 110]. Intra cortical connections may be important to understand the neural computations carried out in V1. Zhaoping has proposed that V1 creates a saliency map using intra cortical mechanisms. This saliency map can be used to attract attention to a visual location without top-down factors, which may explain certain visual search properties [233]. Macknik and Martinez-Conde have proposed that the primary role of feedback may be the maintenance of top-down attention [124, 125].

2.5 Extrastriate Cortex: The Dorsal and Ventral Visual Pathways

The primate cortex has at least 32 distinct visual areas [64, 68] (Fig. 2.12).

In the first two stages of cortical processing (V1 and V2), the magnocellular and the parvocellular pathways are largely segregated: inputs from the LGN arrive to different sublayers in V1 according to their magno/parvo origin and projections from V1 layer 4C are also fairly separated in V1 and V2 as revealed by cytochrome oxidase staining [111, 113, 163, 219]. After V1 there are two main processing streams, associated with different visual capabilities [64, 144, 215]:

- The dorsal or parietal stream is tuned to moving stimuli (with similar properties to the magnocellular pathway). After V2 the information flows to MT, MST and other intermediate areas. MT neurons are selective to the direction of stimulus motion, speed and binocular disparity [4, 13, 229, 230]. The highest stages of this stream are clustered in the posterior parietal cortex. This stream is involved

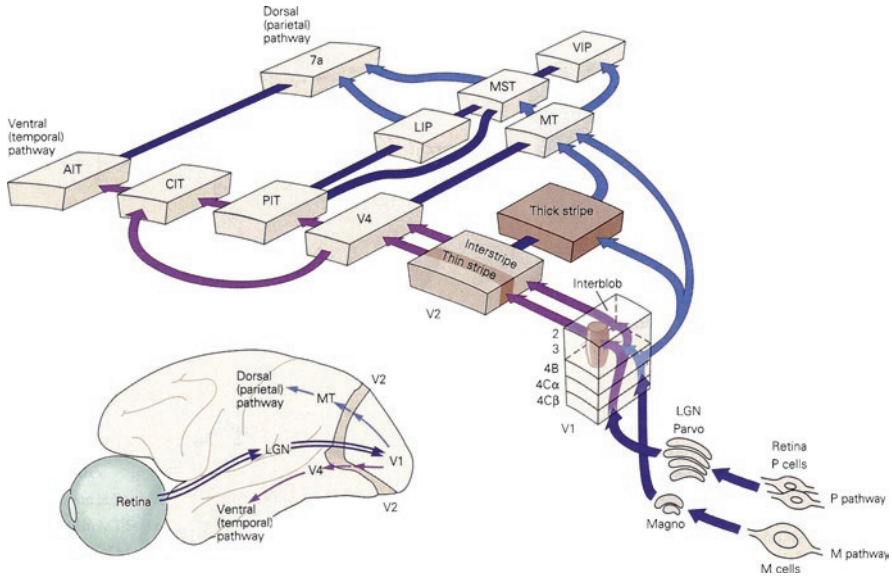


Fig. 2.13 Schematic of the two visual pathways in the primate, showing the main connections between the different areas. From [98]

larger than in V1 [76]. In MST receptive fields can cover a full quadrant of the visual field [63]. V4 receptive fields are about 30 times larger than V1 receptive fields [129, 220], and downstream in the ventral pathway they become over 100 times larger [60].

The hypothesis of two distinct streams of processing was initially formulated by Ungerleider and Mishkin [215]. Many different groups have provided anatomical, physiological, and behavioral support to this idea. In humans, clinical observations indicate that damage to the parietal cortex can affect visual perception of position, leaving object recognition unimpaired [52, 178, 234]. Temporal lobe lesions can produce specific deficits related to object recognition [53, 147, 148, 167]. Systematic lesion studies in primates have found a functional separation between the temporal and the parietal cortices [58, 151, 213].

While it is widely accepted that information is computed in these two largely parallel visual pathways (as shown in schematic on Fig. 2.13 taken from [98]), it is important to note that the separation between the two pathways is far from complete. There is anatomical and physiological evidence of substantial cross-talk between the two streams [68, 149, 218].

2.6 The Role of Spatiotemporal Edges in Early Vision

Information flows from one visual area to the next in the form of excitatory signals carried through glutamate synapses. Therefore, all inhibition between neurons, for instance to form receptive fields, is a function of local inhibitory circuits.

Local inhibition, which underlies center-surround receptive field organization, is enacted through the neurotransmitter GABA (gamma-aminobutyric acid). In 1965 Hartline and Ratliff delineated the far-reaching consequences of this simple arrangement, in terms of spatial and temporal visual processing [179]. They showed that the three components of a laterally inhibitory circuit:

1. Excitatory input and output: information arrives at a given visual area of the brain in the form of excitatory neural responses, and the information is sent to the next visual area(s) in the visual hierarchy as excitatory neural responses as well.
2. Lateral inhibition: occurs as a function of excitatory activation (thus inhibition follows excitation in time).
3. Self-inhibition: neurons that laterally inhibit their neighbors also inhibit themselves.

Figure 2.14 shows a plausible mammalian descriptive model of lateral inhibition, based on Hartline and Ratliff's original Limulus model [123]. The model predicts

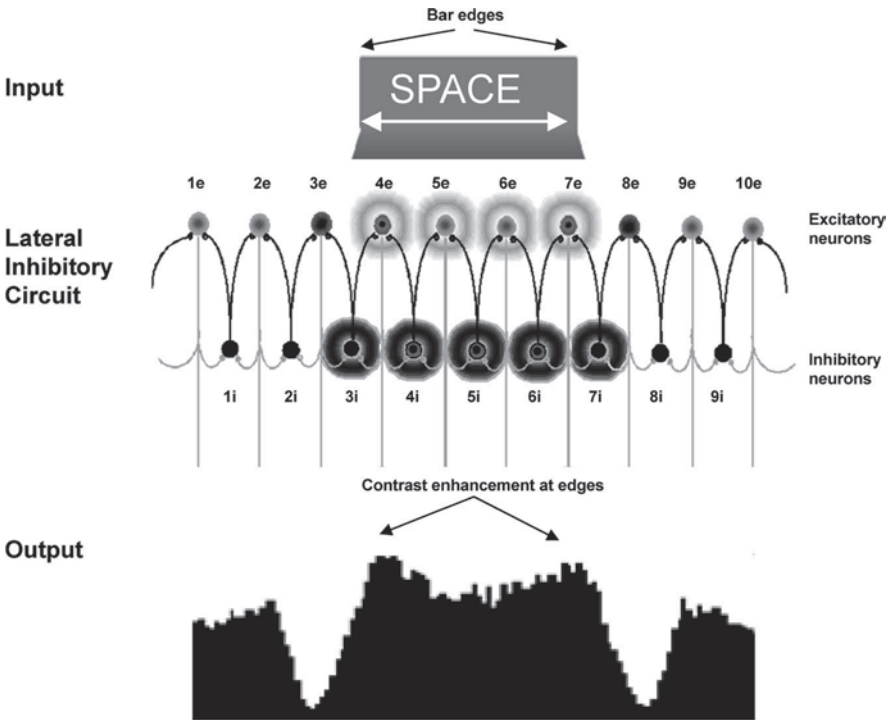


Fig. 2.14 A mammalian representation of the spatial lateral inhibition model originally proposed by Hartline and Ratliff. The excitatory neurons in the center of the upper row receive excitatory input from a visual stimulus. This excitation is transmitted laterally to the inhibitory neurons just outside the stimulus, and also within the area impinged upon by the stimulus. The inhibitory interactions between excited neurons at the edges of stimuli and their non-excited neighbors results in apparent contrast enhancement at the borders of the stimulus. Output of each of the excitatory neurons is represented in action potentials per unit time at the bottom [127]

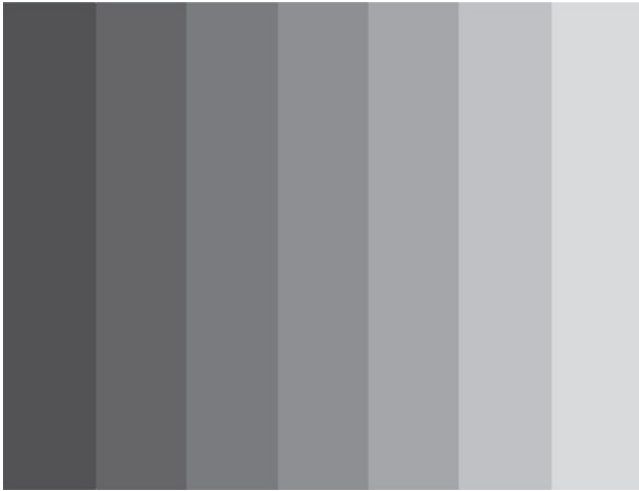


Fig. 2.15 This Mach Band demonstration was originally designed by Chevreul in 1839. Notice how each vertical stripe appears to be lighter on the left than on the right. This illusory effect is due to contrast enhancement at the borders

that the strongest neural excitatory signals to a visual stimulus will occur just inside the stimulus' spatial borders. Neural inhibition, moreover, is strongest just outside of the borders. The spatial interiors of stimuli do not cause responses in visual neurons. It is hypothesized that the interiors of large spatial stimuli are visible through the illusory process of filling-in. One perceptual consequence of lateral inhibition is that stimuli to both sides of a luminance border are differentially enhanced in an illusory fashion (as in Fig. 2.15).

If we now examine two of the neurons in a lateral inhibitory network through time, one neuron being excitatory and the other inhibitory, we should expect the following specific temporal pattern of response (Fig. 2.16). Visual information enters a given visual area as excitatory input to specific neurons that are tuned to the specific visual stimulus being presented. The excited neurons then locally inhibit their neighbors, and also themselves, in a delayed inhibitory response that serves to bring suppress the initial transient onset-response. This state of excitatory-inhibitory equilibrium continues until such point that the excitatory input representing the stimulus is extinguished. After that point, the neurons briefly enter a state of suppression due to the fact that delayed inhibition is unopposed by excitation (a refractory period called the time-out), followed by a disinhibitory rebound, called an after-discharge. Just as neurons respond strongly to the spatial borders of stimuli due to lateral inhibition, so too do they respond strongly to the temporal borders (the stimulus onsets and terminations (also commonly called "stimulus offsets," although this term is linguistically incorrect)). The perceptual result of this is contrast enhancement at the temporal borders of stimuli. Lateral inhibition is thus responsible not only for the spatial layout of receptive fields, but also for their temporal response properties. The perceptual result of this process is that the perceived

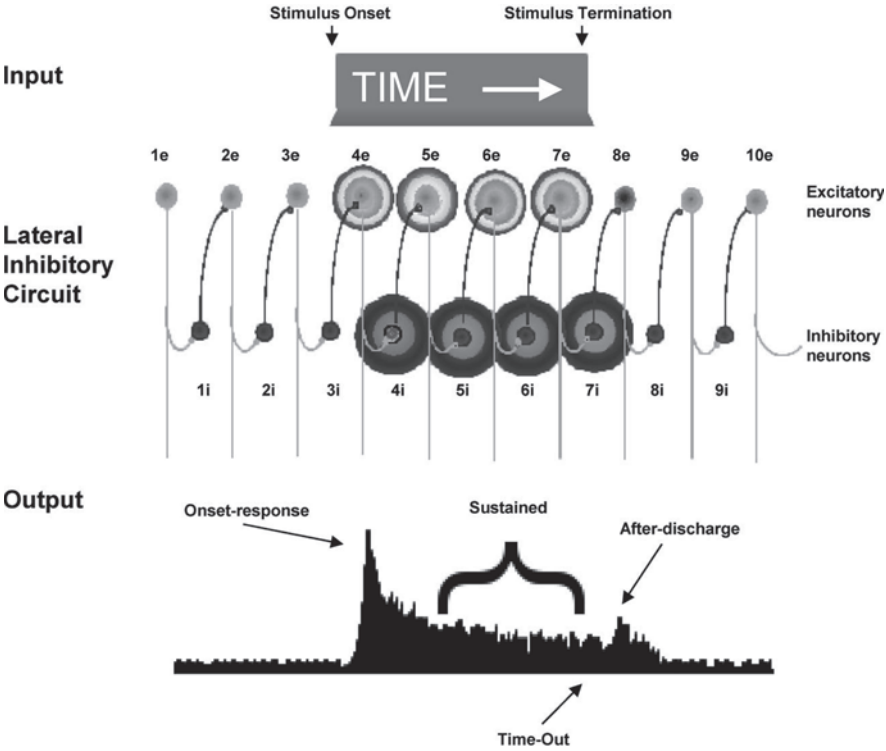


Fig. 2.16 One excitatory and one inhibitory neuron, followed through a period of time in which the stimulus is off (times 1, 2 and 3), on (times 4, 5, 6, and 7), and then off (times 8, 9 and 10) [127]

contrast of a stimulus is highest just after it turns on and then again after it turns off. Visual masking (the effect in which the visibility of a target stimulus is reduced by a masking stimulus that does not overlap the target in space or time) occurs perceptually when the neural responses to the target onset and/or termination are inhibited, suggesting that the onset-response and after-discharge are critical for the visibility of stimuli [120, 122, 126].

2.7 The Role of Corners in Early Vision

2.7.1 Overview

Our perception of the visual world is constructed, step-by-step, by neurons in different visual areas of the brain [59, 68, 91, 195]. While feedback certainly plays a role in the visual system [6, 7, 96, 124, 125, 133, 157], the visual system's overall

tendency is towards a hierarchy, in which neurons in sequential levels extract more and more complicated features from the visual scene. These features include (but are not limited to) color, brightness, movement, shape, and depth.

In order to determine how visual perception is constructed in our brain, we need first to establish the nature of the fundamental visual features in a scene. Theories of shape and brightness perception have primarily focused on the detection and processing of visual edges. Early visual neurons are thought of as “edge detectors” [91, 132], and current studies are based on the assumption that edges are the most elementary visual feature. However, recent experiments show that corners can be more salient than edges, both perceptually (Fig. 2.17) [206, 208] and in the responses

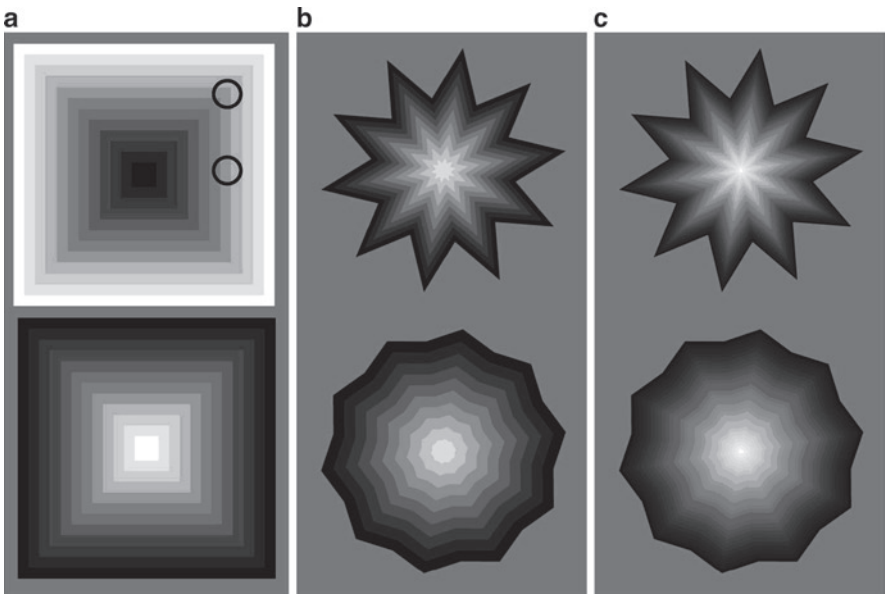


Fig. 2.17 Vasarely’s nested squares and alternating brightness star illusions. **(a)** Nested squares illusion, based in Vasarely’s “Arcturus” [221]. *Top*: The stimulus is made out of multiple concentric squares of increasing luminance (going from *black* in the center to *white* in the outside). The two circles indicate two regions that appear to have significantly different brightness. The area inside the upper circle has higher average luminance than the region inside the lower circle; however the region inside the upper circle appears perceptually darker. *Bottom*: Nested square stimulus, with a gradient of decreasing luminance (from the center to the outside). From [206]. **(b, c)** The Alternating Brightness Star illusion [134]. The stimulus is made of concentric stars of graded luminance. In the examples illustrated, the innermost star is white; the outermost star is black. The illusory corner-folds that radiate from the center appear as light or dark depending on the polarity of the corner angle; Corner Angle Brightness Reversal effect. Moreover, the illusory folds appear more salient with sharp corners (*top stars*), and less salient with shallow corners (*bottom stars*); Corner Angle Brightness Variation effect. However, all illusory folds are physically equal to each other in luminance. **(b)** The gradient from the center to the outside has ten luminance steps, and so the individual stars forming the polygonal constructs are easy to identify. **(c)** The gradient from the center to the outside has 100 luminance steps. From [208]

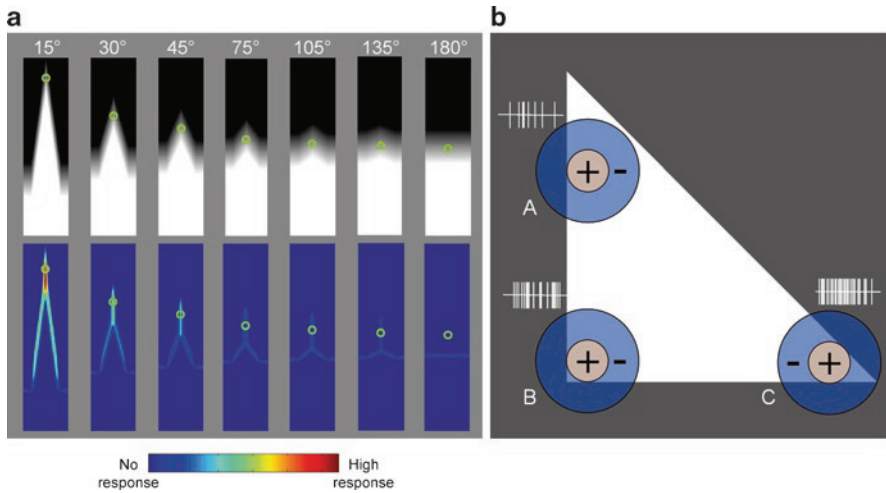


Fig. 2.18 Center-surround receptive field responses to corners of varying angles. **(a)** Computational simulations with a DOG filter. The filter parameters were chosen to match physiological center-surround receptive fields at the eccentricity used in the psychophysical experiments (3°). *Top*: Examples of corner-gradient stimuli analyzed in the simulations. The circles mark the point of 50% luminance. *Bottom*: Convolution of the DOG filter with the stimuli in (A) simulates the output of an array of center-surround neurons. The circles indicate the responses of the model at the point of 50% luminance on the actual gradient. **(b)** Generalized model of corner processing. Three on-center receptive fields are respectively placed over one edge and two corners of a *white triangle*. The center of the receptive field over the edge (position A) is well stimulated by light, but most of the surround also falls in the light region, so the response of the neuron is partially inhibited. The center of the receptive field over the 90° corner (position B) is also stimulated by light and most of the surround falls in the dark area. This is a more optimal stimulus than in (A) and leads to a stronger neural response. The receptive field over the 45° corner (position C) receives even more optimal contrast between center and surround, leading to an even stronger response. The spiking responses depicted in the cartoon are hypothetical. From [206]

of neurons throughout the visual hierarchy, even in early stages (Fig. 2.18) [206, 210]. Combined results from human psychophysics experiments, human brain imaging, and computational modeling suggest that deflections or discontinuities in edges, such as corners, curvature, and terminating line endings, may be first processed by center-surround receptive fields [206, 208, 210]. These data suggest that corners may be a fundamental feature for shape and brightness perception.

This hypothesis in no way rules out a critical role for later cortical areas in more complex processing of corner angles. For instance, specific orientations of corner angles must be processed cortically, given that the first orientation-selective cells are cortical.

2.7.2 Corner Perception and the Redundancy-Reducing Hypothesis

The information transmitted by our visual system is constrained by physical limitations, such as the relatively small number of axons available in the optic nerve. To some extent, our visual system overcomes these limitations by extracting, emphasizing, and processing non-redundant visual features. In 1961, Barlow proposed that the brain recodes visual data “so that their redundancy is reduced but comparatively little information is lost.” This idea is known as the “Redundancy-Reducing Hypothesis” [14, 15]. The redundancy-reducing hypothesis has been invoked as an explanation for why neurons at the early levels of the visual system are suited to perform “edge-detection,” or “contour-extraction.” However, redundancy reduction is not necessarily constrained to edges, but rather should theoretically apply to any feature in the visual scene [177]. Just as edges are a less redundant feature than diffuse light, Fred Attneave proposed in the 1950s that “points of maximum curvature” (i.e., discontinuities in edges, such as curves, angles and corners – any point at which straight-lines are deflected) are even less redundant than edges themselves, and thus contain more information [12]. If points of high curvature are less redundant than points of low curvature, then sharp corners should also be less redundant than shallow corners. This hypothesis is consistent with experiments showing that sharp corners are perceptually more salient and generate stronger physiological responses than shallow corners [206, 208, 210].

2.8 Effects of Fixational Eye Movements in Early Visual Physiology and Perception

2.8.1 Overview

As we read a page of text, our eyes rapidly flick from left to right in small hops, bringing each word sequentially into focus. When we look at a person’s face, our eyes similarly dart here and there, resting momentarily on one eye, the other eye, mouth and other features. But these large eye movements, called saccades (Fig. 2.19a), are just a small part of the daily workout our eye muscles get. Our eyes *never* stop moving: even when they are apparently fixated on something, they still jump and jiggle imperceptibly in ways that turn out to be essential for seeing. The tiny eye motions that we produce whenever we fixate our gaze are called fixational eye movements (Fig. 2.19b) [139]. If these miniature motions are halted during fixation, all stationary objects simply fade from view.

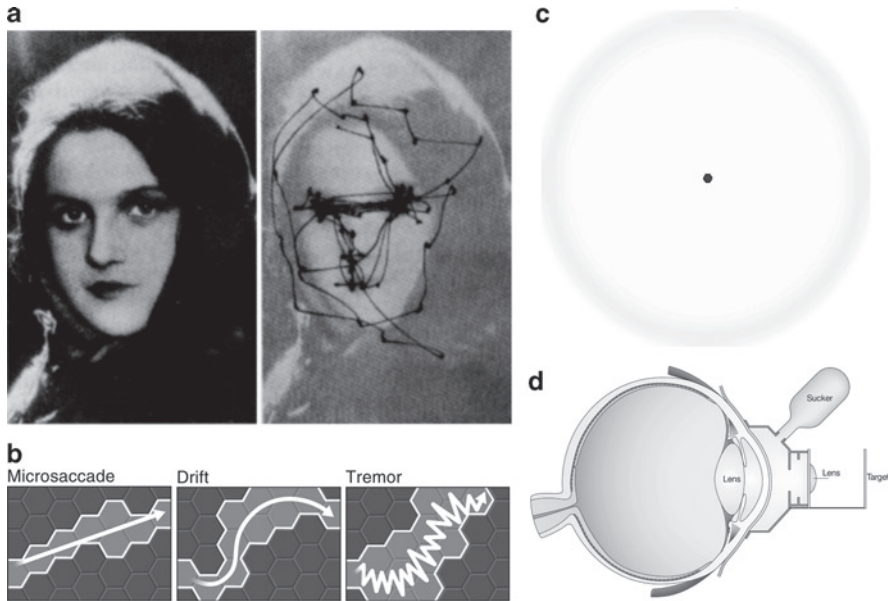


Fig. 2.19 Fixational eye movements and visual fading. **(a)** An observer views a picture (*left*) while eye positions are monitored (*right*). The eyes jump, seem to fixate or rest momentarily, producing a small dot on the trace, then jump to a new region of interest. The large jumps in eye position illustrated here are called saccades. However, even during fixation, or “rest” times, eyes are never still, but continuously produce fixational eye movements: drifts, tremor, and microsaccades. From [228]. **(b)** Cartoon representation of fixational eye movements in humans and primates. Microsaccades (straight and fast movements), drifts (curvy slow movements) and tremor (oscillations superimposed on drifts) transport the visual image across the retinal photoreceptor mosaic. From [135]. **(c)** Troxler fading. In 1804 Swiss philosopher Ignaz Paul Vital Troxler discovered that deliberately fixating on something causes surrounding stationary images to fade away. To elicit this experience, stare at the central dot while paying attention to the surrounding pale ring. The ring soon vanishes, and the central dot appears set against a white background. Move your eyes, and it pops back into view. Modified from [139]. **(d)** This drawing illustrates the suction cup technique, used by Yarbus [228] and others. This technique was very popular in early retinal stabilization studies for its simplicity, but it is now considered old-fashioned, and other, less invasive stabilization techniques are preferred. The target image is directly attached to the eyeball by means of a contact lens assembly. The target is viewed through a powerful lens. The assembly is firmly attached to the eye by a suction device. Modified from [139]

2.8.2 Neural Adaptation and Visual Fading

That the eyes move constantly has been known for centuries. In 1860 Hermann von Helmholtz pointed out that keeping one’s eyes motionless was a difficult proposition and suggested that “wandering of the gaze” prevented the retina from becoming tired.

Animal nervous systems may have evolved to detect changes in the environment, because spotting differences promotes survival. Motion in the visual field

may indicate that a predator is approaching or that prey is escaping. Such changes prompt visual neurons to respond with neural impulses. Unchanging objects do not generally pose a threat, so animal brains – and visual systems – did not evolve to notice them. Frogs are an extreme case, as they produce no spontaneous eye movements in the absence of head movements. For a resting frog, such lack of eye movements results in the visual fading of all stationary objects. Jerome Lettvin and colleagues stated that a frog “will starve to death surrounded by food if it is not moving.” Thus a fly sitting still on the wall will be invisible to a resting frog, but once the fly is aloft, the frog will immediately detect it and capture it with its tongue.

Frogs cannot see unmoving objects because an unchanging stimulus leads to “neural adaptation.” That is, under constant stimulation, visual neurons adjust their gain as to gradually stop responding. Neural adaptation saves energy but also limits sensory perception. Human neurons also adapt to sameness. However, the human visual system does much better than a frog’s at detecting unmoving objects, because human eyes create their own motion, even during visual fixation. Fixational eye movements shift the visual scene across the retina, prodding visual neurons into action and counteracting neural adaptation. They thus prevent stationary objects from fading away.

The goal of oculomotor fixational mechanisms may not be retinal stabilization, but rather controlled image motion adjusted so as to overcome adaptation in an optimal fashion for visual processing [198].

In 1804, Troxler reported that precisely fixating the gaze on an object of interest causes stationary images in the surrounding region gradually to fade away. Thus, even a small reduction in the rate and size of fixational eye movements greatly impairs vision, even outside of the laboratory and for observers with healthy eyes and brains (Fig. 2.19c).

Eliminating *all* eye movements, however, can only be achieved in a laboratory. In the early 1950s, some research teams achieved this stilling effect with a tiny custom slide projector, mounted directly onto a contact lens that attached directly to the observer’s eye with a suction device (Fig. 2.19d). In this setup, a person views the projected image through this lens, which moves with the eye. Using such a retinal stabilization technique, the image shifts every time the eye shifts. Thus it remains still with respect to the eye, causing the visual neurons to adapt and the image to fade away. Nowadays, researchers create this same result by measuring eye movements with a camera pointed at the eye. They transmit the eye-position data to a projection system that moves the image with the eye, thereby stabilizing the image on the retina.

Around the same time, three different types of fixational eye movements were characterized. *Microsaccades* are small, involuntary saccades that are produced when the subjects attempt to fixate their gaze on a visual target. They are the largest and fastest of the fixational eye movements, carrying an image across dozens to several hundreds of photoreceptors. *Drifts* are slow meandering motions that occur between the fast, linear microsaccades. *Tremor* is a tiny, very fast oscillation superimposed on drifts. Tremor is the smallest type of fixational eye movement, its motion no bigger than the size of one photoreceptor. See Martinez-Conde et al. [136, 139, 141] for some recent reviews of fixational eye movement parameters in humans, primates, and other vertebrates.

2.8.3 *Microsaccades in Visual Physiology and Perception*

Starting in the late 1990s, fixational eye movement research has focused on microsaccades. Physiological experiments found that microsaccades increase the firing of neurons in the visual cortex and lateral geniculate nucleus, by moving the images of stationary stimuli in and out of neuronal receptive fields. Firing rate increases following microsaccades were clustered in bursts of spikes, whereas individual spikes tended to occur in the periods between microsaccades. Moreover, bursts of spikes were better correlated with previous microsaccades than either single spikes or instantaneous firing rate. Bursts highly correlated with previous microsaccades had large spike numbers and short inter-spike intervals [137, 138]. Because microsaccades are related to maintaining visibility and counteracting fading (see further below), bursts that indicate previous microsaccades accurately must encompass the neural code for visibility. In area V1, optimal burst sizes following microsaccades tended to be three spikes or more. These bursts may be an important clue to the neural code or “language” that our brain uses to represent the visibility of the world [137]. The neural codes by which neurons, or neuronal populations, encode and transmit visual information are not only critical to our understanding of normal visual processing, but also to the development and refinement of neural prostheses.

Microsaccades could enhance spatial summation by synchronizing the activity of nearby neurons [137]. By generating bursts of spikes, microsaccades may also enhance temporal summation of responses from neurons with neighboring RFs [137]. Moreover, microsaccades may help disambiguate latency and brightness in visual perception, allowing us to use latency in our visual discriminations [137]. Changes in contrast can be encoded as changes in the latency of neuronal responses [2, 3, 77]. Since the brain knows when a microsaccade is generated, differential latencies in visual responses could be used by the brain to indicate differences in contrast and salience.

Despite several decades of debate (see [139] for a review), a direct link between microsaccade production and visual perception has only recently been demonstrated. Martinez-Conde et al. [140] found that increased microsaccade production during fixation resulted in enhanced visibility for visual targets. Conversely, decreased microsaccade production led to periods of visual fading. These results established a potential causal relationship between microsaccades and target visibility during fixation, and corroborated predictions from previous physiological studies in which microsaccades were found to increase the spiking rates in visual neurons [137, 138]. Microsaccade production has been subsequently linked to perceptual transitions in various other visual phenomena, such as binocular rivalry [215], filling-in of artificial scotomas [207], and illusory motion (perceived speed as well as subjective direction [108, 209]).

Fewer studies have addressed the neural and perceptual consequences of drifts and tremor. However, all fixational eye movements may contribute significantly to visual perception, depending on stimulation conditions. For example, receptive fields in the periphery may be so large that only microsaccades are large and fast

enough – compared to drifts and tremor – to prevent visual fading, especially with low-contrast stimuli. Whereas foveal receptive fields may be so small that drifts and tremor can maintain vision in the absence of microsaccades. But even if drifts and/or tremor can maintain foveal vision on their own, this does not rule out that microsaccades could also have a role. Thus, if one were to eliminate drifts and tremor, microsaccades alone might sustain foveal vision during fixation.

References

1. Ahnelt PK, Kolb H, Pflug R (1987), *Identification of a subtype of cone photoreceptor, likely to be blue sensitive, in the human retina*. J Comp Neurol, **255**(1): p. 18–34.
2. Albrecht DG (1995), *Visual cortex neurons in monkey and cat: effect of contrast on the spatial and temporal phase transfer functions*. Vis Neurosci, **12**(6): p. 1191–210.
3. Albrecht DG, Hamilton DB (1982), *Striate cortex of monkey and cat: contrast response function*. J Neurophysiol **48**: p. 217–37.
4. Albright TD (1984), *Direction and orientation selectivity of neurons in visual area MT of the macaque*. J Neurophysiol, **52**(6): p. 1106–30.
5. Alitto HJ, Usrey WM (2003), *Corticothalamic feedback and sensory processing*. Curr Opin Neurobiol, **13**(4): p. 440–5.
6. Alonso JM, Cudeiro J, Perez R, et al. (1993), *Influence of layer V of area 18 of the cat visual cortex on responses of cells in layer V of area 17 to stimuli of high velocity*. Exp Brain Res, **93**(2): p. 363–6.
7. Alonso JM, Cudeiro J, Perez R, et al. (1993), *Orientational influences of layer V of visual area 18 upon cells in layer V of area 17 in the cat cortex*. Exp Brain Res, **96**(2): p. 212–20.
8. Alonso JM, Martinez LM (1998), *Functional connectivity between simple cells and complex cells in cat striate cortex*. Nat Neurosci, **1**(5): p. 395–403.
9. Alonso JM, Usrey WM, Reid RC (2001), *Rules of connectivity between geniculate cells and simple cells in cat primary visual cortex*. J Neurosci, **21**(11): p. 4002–15.
10. Anderson JC, Martin KA, Whitteridge D (1993), *Form, function, and intracortical projections of neurons in the striate cortex of the monkey Macacus nemestrinus*. Cereb Cortex, **3**(5): p. 412–20.
11. Angelucci A, Levitt JB, Walton EJ, et al. (2002), *Circuits for local and global signal integration in primary visual cortex*. J Neurosci, **22**(19): p. 8633–46.
12. Attneave F (1954), *Some informational aspects of visual perception*. Psychol Rev, **61**(3): p. 183–93.
13. Baker JF, Petersen SE, Newsome WT, Allman JM (1981), *Visual response properties of neurons in four extrastriate visual areas of the owl monkey (Aotus trivirgatus): a quantitative comparison of medial, dorsomedial, dorsolateral, and middle temporal areas*. J Neurophysiol, **45**(3): p. 397–416.
14. Barlow HB (1961), *Possible principles underlying the transformation of sensory messages, in Sensory Communication*, Rosenblith WA, Editor. MIT Press: Cambridge, MA. p. 217–34.
15. Barlow HB (1989), *Unsupervised learning*. Neural Computation, **1**: p. 295–311.
16. Barlow HB, Fitzhugh R, Kuffler SW (1957), *Change of organization in the receptive fields of the cat's retina during dark adaptation*. J Physiol, **137**: p. 228–54.
17. Barone P, Batardiere A, Knoblauch K, Kennedy H (2000), *Laminar distribution of neurons in extrastriate areas projecting to visual areas V1 and V4 correlates with the hierarchical rank and indicates the operation of a distance rule*. J Neurosci, **20**(9): p. 3263–81.
18. Bauer R, Dow BM, Vautin RG (1980), *Laminar distribution of preferred orientations in foveal striate cortex of the monkey*. Exp Brain Res, **41**(1): p. 54–60.

19. Benevento LA, Standage GP (1982), *Demonstration of lack of dorsal lateral geniculate nucleus input to extrastriate areas MT and visual 2 in the macaque monkey*. Brain Res, **252**(1): p. 161–6.
20. Blasdel G, Obermayer K, Kiorpes L (1995), *Organization of ocular dominance and orientation columns in the striate cortex of neonatal macaque monkeys*. Vis Neurosci, **12**(3): p. 589–603.
21. Blasdel GG, Fitzpatrick D (1984), *Physiological organization of layer 4 in macaque striate cortex*. J Neurosci, **4**(3): p. 880–95.
22. Blasdel GG, Lund JS (1983), *Termination of afferent axons in macaque striate cortex*. J Neurosci, **3**(7): p. 1389–413.
23. Blasdel GG, Lund JS, Fitzpatrick D (1985), *Intrinsic connections of macaque striate cortex: axonal projections of cells outside lamina 4C*. J Neurosci, **5**(12): p. 3350–69.
24. Blasdel GG, Salama G (1986), *Voltage-sensitive dyes reveal a modular organization in monkey striate cortex*. Nature, **321**(6070): p. 579–85.
25. Bolz J, Gilbert CD (1986), *Generation of end-inhibition in the visual cortex via interlaminar connections*. Nature, **320**(6060): p. 362–5.
26. Bonhoeffer T, Grinvald A (1991), *Iso-orientation domains in cat visual cortex are arranged in pinwheel-like patterns*. Nature, **353**(6343): p. 429–31.
27. Bonin V, Mante V, Carandini M (2005), *The suppressive field of neurons in lateral geniculate nucleus*. J Neurosci, **25**(47): p. 10844–56.
28. Bowling DB (1980), *Light responses of ganglion cells in the retina of the turtle*. J Physiol, **299**: p. 173–96.
29. Boycott BB, Dowling JE (1969), *Organization of the primate retina: light microscopy*. Philos Trans R Soc Lond B Biol Sci, **B, 255**: p. 109–84.
30. Boycott BB, Wässle H (1991), *Morphological Classification of Bipolar Cells of the Primate Retina*. Eur J Neurosci, **3**(11): p. 1069–88.
31. Brodmann K (1909), *Vergleichende Lokalisationlehre der Grosshirnrinde in ihren Prinzipien-Dargestellt auf Grund des Zellenbaues*. Leipzig: Barth.
32. Brown PK, Wald G (1963), *Visual pigments in human and monkey retinas*. Nature, **200**: p. 37–43.
33. Brown PK, Wald G (1964), *Visual Pigments In Single Rods And Cones Of The Human Retina. Direct Measurements Reveal Mechanisms Of Human Night And Color Vision*. Science, **144**: p. 45–52.
34. Bullier J, Henry GH (1980), *Ordinal position and afferent input of neurons in monkey striate cortex*. J Comp Neurol, **193**(4): p. 913–35.
35. Bullier J, Kennedy H (1983), *Projection of the lateral geniculate nucleus onto cortical area V2 in the macaque monkey*. Exp Brain Res, **53**(1): p. 168–72.
36. Callaway EM (1998), *Local circuits in primary visual cortex of the macaque monkey*. Annu Rev Neurosci, **21**: p. 47–74.
37. Callaway EM, Wiser AK (1996), *Contributions of individual layer 2–5 spiny neurons to local circuits in macaque primary visual cortex*. Vis Neurosci, **13**(5): p. 907–22.
38. Carandini M (2004), *Receptive fields and suppressive fields in the early visual system*, in *The cognitive neurosciences*, Gazzaniga MS, Editor. MIT Press: Cambridge, MA.
39. Carandini M, Heeger DJ, Movshon JA (1997), *Linearity and normalization in simple cells of the macaque primary visual cortex*. J Neurosci, **17**(21): p. 8621–44.
40. Chance FS, Nelson SB, Abbot LF (1999), *Complex cells as cortically amplified simple cells*. Nature Neurosci, **2**: p. 277–82.
41. Cicerone CM, Nerger JL (1989), *The relative numbers of long-wavelength-sensitive to middle-wavelength-sensitive cones in the human fovea centralis*. Vision Res, **29**(1): p. 115–28.
42. Conley M, Fitzpatrick D (1989), *Morphology of retinogeniculate axons in the macaque*. Vis Neurosci, **2**(3): p. 287–96.
43. Crair MC, Ruthazer ES, Gillespie DC, Stryker MP (1997), *Ocular dominance peaks at pinwheel center singularities of the orientation map in cat visual cortex*. J Neurophysiol, **77**(6): p. 3381–5.

44. Curcio CA, Allen KA, Sloan KR, et al. (1991), *Distribution and morphology of human cone photoreceptors stained with anti-blue opsin*. J Comp Neurol, **312**(4): p. 610–24.
45. Curcio CA, Sloan KR, Jr., Packer O, et al. (1987), *Distribution of cones in human and monkey retina: individual variability and radial asymmetry*. Science, **236**(4801): p. 579–82.
46. Curcio CA, Sloan KR, Kalina RE, Hendrickson AE (1990), *Human photoreceptor topography*. J Comp Neurol, **292**(4): p. 497–523.
47. Dacey D, Packer OS, Diller L, et al. (2000), *Center surround receptive field structure of cone bipolar cells in primate retina*. Vision Res, **40**(14): p. 1801–11.
48. Dacey DM (1993), *The mosaic of midget ganglion cells in the human retina*. J Neurosci, **13**(12): p. 5334–55.
49. Dacey DM (1999), *Primate retina: cell types, circuits and color opponency*. Prog Retin Eye Res, **18**(6): p. 737–63.
50. Dacey DM (2000), *Parallel pathways for spectral coding in primate retina*. Annu Rev Neurosci, **23**: p. 743–75.
51. Dacey DM, Petersen MR (1992), *Dendritic field size and morphology of midget and parasol ganglion cells of the human retina*. Proc Natl Acad Sci USA, **89**(20): p. 9666–70.
52. Damasio AR, Benton AL (1979), *Impairment of hand movements under visual guidance*. Neurology, **29**(2): p. 170–4.
53. Damasio AR, Damasio H, Van Hoesen GW (1982), *Prosopagnosia: anatomic basis and behavioral mechanisms*. Neurology, **32**(4): p. 331–41.
54. Das A, Gilbert CD (1999), *Topography of contextual modulations mediated by short-range interactions in primary visual cortex*. Nature, **399**(6737): p. 655–61.
55. De Monasterio FM, Gouras P (1975), *Functional properties of ganglion cells of the rhesus monkey retina*. J Physiol, **251**(1): p. 167–95.
56. de Monasterio FM, Schein SJ (1982), *Spectral bandwidths of color-opponent cells of geniculocortical pathway of macaque monkeys*. J Neurophysiol, **47**(2): p. 214–24.
57. De Valois RL (1960), *Color vision mechanisms in the monkey*. J Gen Physiol, **43**(6): p. 115–28.
58. Dean P (1976), *Effects of inferotemporal lesions on the behavior of monkeys*. Psychol Bull, **83**(1): p. 41–71.
59. Desimone R, Fleming J, Gross CG (1980), *Prestriate afferents to inferior temporal cortex: an HRP study*. Brain Res, **184**(1): p. 41–55.
60. Desimone R, Gross CG (1979), *Visual areas in the temporal cortex of the macaque*. Brain Res, **178**(2–3): p. 363–80.
61. Desimone R, Schein SJ (1987), *Visual properties of neurons in area V4 of the macaque: sensitivity to stimulus form*. J Neurophysiol, **57**(3): p. 835–68.
62. Desimone R, Schein SJ, Moran J, Ungerleider LG (1985), *Contour, color and shape analysis beyond the striate cortex*. Vision Res, **25**(3): p. 441–52.
63. Desimone R, Ungerleider LG (1986), *Multiple visual areas in the caudal superior temporal sulcus of the macaque*. J Comp Neurol, **248**(2): p. 164–89.
64. Desimone R, Ungerleider LG (1989), *Neural mechanisms of visual processing in monkeys*, in *Handbook of neuropsychology*, Boller F, Graman J, Editors. Elsevier: Amsterdam. p. 267–99.
65. Donner KO, Reuter T (1965), *The dark-adaptation of single units in the frog's retina and its relation to the regeneration of rhodopsin*. Vision Res, **5**(11): p. 615–32.
66. Dowling JE, Boycott BB (1966), *Organization of the primate retina: electron microscopy*. Proc R Soc Lond B Biol Sci, **166**(2): p. 80–111.
67. Erisir A, Van Horn SC, Sherman SM (1997), *Relative numbers of cortical and brainstem inputs to the lateral geniculate nucleus*. Proc Natl Acad Sci USA, **94**(4): p. 1517–20.
68. Felleman DJ, Van Essen DC (1991), *Distributed hierarchical processing in the primate cerebral cortex*. Cereb Cortex, **1**(1): p. 1–47.
69. Ferster D, Chung S, Wheat H (1996), *Orientation selectivity of thalamic input to simple cells of cat visual cortex*. Nature, **380**(6571): p. 249–52.
70. Ferster D, Koch C (1987), *Neuronal connections underlying orientation selectivity in cat visual cortex*. Trends Neurosci, **10**: p. 487–92.
71. Ferster D, Miller KD (2000), *Neural mechanisms of orientation selectivity in the visual cortex*. Annu Rev Neurosci, **23**: p. 441–71.

72. Fitzpatrick D, Lund JS, Blasdel GG (1985), *Intrinsic connections of macaque striate cortex: afferent and efferent connections of lamina 4C*. J Neurosci, **5**(12): p. 3329–49.
73. Fitzpatrick D, Usrey WM, Schofield BR, Einstein G (1994), *The sublaminal organization of corticogeniculate neurons in layer 6 of macaque striate cortex*. Vis Neurosci, **11**(2): p. 307–15.
74. Gallant JL, Braun J, Van Essen DC (1993), *Selectivity for polar, hyperbolic, and Cartesian gratings in macaque visual cortex*. Science, **259**(5091): p. 100–3.
75. Gallant JL, Connor CE, Rakshit S, et al. (1996), *Neural responses to polar, hyperbolic, and Cartesian gratings in area V4 of the macaque monkey*. J Neurophysiol, **76**(4): p. 2718–39.
76. Gattass R, Gross CG (1981), *Visual topography of striate projection zone (MT) in posterior superior temporal sulcus of the macaque*. J Neurophysiol, **46**(3): p. 621–38.
77. Gawne TJ, Kjaer TW, Richmond BJ (1996), *Latency: another potential code for feature binding in striate cortex*. J Neurophysiol, **76**(2): p. 1356–60.
78. Gilbert CD (1977), *Laminar differences in receptive field properties of cells in cat primary visual cortex*. J Physiol, **268**(2): p. 391–421.
79. Gilbert CD, Das A, Ito M, et al. (1996), *Spatial integration and cortical dynamics*. Proc Natl Acad Sci USA, **93**(2): p. 615–22.
80. Gilbert CD, Wiesel TN (1979), *Morphology and intracortical projections of functionally characterised neurones in the cat visual cortex*. Nature, **280**(5718): p. 120–5.
81. Gilbert CD, Wiesel TN (1983), *Clustered intrinsic connections in cat visual cortex*. J Neurosci, **3**(5): p. 1116–33.
82. Gouras P (1968), *Identification of cone mechanisms in monkey ganglion cells*. J Physiol, **199**(3): p. 533–47.
83. Guillery RW, Sherman SM (2002), *Thalamic relay functions and their role in corticocortical communication: generalizations from the visual system*. Neuron, **33**(2): p. 163–75.
84. Gur M, Kagan I, Snodderly DM (2005), *Orientation and direction selectivity of neurons in V1 of alert monkeys: functional relationships and laminar distributions*. Cereb Cortex, **15**(8): p. 1207–21.
85. Hendrickson AE, Wilson JR, Ogren MP (1978), *The neuroanatomical organization of pathways between the dorsal lateral geniculate nucleus and visual cortex in Old World and New World primates*. J Comp Neurol, **182**(1): p. 123–36.
86. Hendry SH, Reid RC (2000), *The koniocellular pathway in primate vision*. AnnuRev Neurosci, **23**: p. 127–53.
87. Hendry SH, Yoshioka T (1994), *A neurochemically distinct third channel in the macaque dorsal lateral geniculate nucleus*. Science, **264**(5158): p. 575–7.
88. Hubel DH (1995), *Eye, brain and vision*. 2ed. New York: Scientific American Library. 242.
89. Hubel DH, Wiesel TN (1959), *Receptive fields of single neurones in the cat's striate cortex*. J Physiol, **148**: p. 574–91.
90. Hubel DH, Wiesel TN (1961), *Integrative action in the cat's lateral geniculate body*. J Physiol, **155**: p. 385–98.
91. Hubel DH, Wiesel TN (1962), *Receptive fields, binocular interaction and functional architecture in the cat's visual cortex*. J Physiol, **160**: p. 106–54.
92. Hubel DH, Wiesel TN (1965), *Receptive fields and functional architecture in two nonstriate visual areas (18 and 19) of the cat*. J Neurophysiol, **28**: p. 229–89.
93. Hubel DH, Wiesel TN (1968), *Receptive fields and functional architecture of monkey striate cortex*. J Physiol, **195**(1): p. 215–43.
94. Hubel DH, Wiesel TN (1972), *Laminar and columnar distribution of geniculo-cortical fibers in the macaque monkey*. J Comp Neurol, **146**(4): p. 421–50.
95. Hubel DH, Wiesel TN (1974), *Sequence regularity and geometry of orientation columns in the monkey striate cortex*. J Comp Neurol, **158**(3): p. 267–93.
96. Hupe JM, James AC, Payne BR, et al. (1998), *Cortical feedback improves discrimination between figure and background by V1, V2 and V3 neurons*. Nature, **394**(6695): p. 784–7.
97. Jones HE, Grieve KL, Wang W, Sillito AM (2001), *Surround suppression in primate V1*. J Neurophysiol, **86**(4): p. 2011–28.
98. Kandel ER, Schwartz JH, Jessell TM, eds (2000). *Principles of neural science*. 4th ed. McGraw Hill: New York.

99. Kaneko A (1970), *Physiological and morphological identification of horizontal, bipolar and amacrine cells in goldfish retina*. J Physiol, **207**(3): p. 623–33.
100. Kapadia MK, Westheimer G, Gilbert CD (1999), *Dynamics of spatial summation in primary visual cortex of alert monkeys*. Proc Natl Acad Sci USA, **96**(21): p. 12073–8.
101. Kaplan E, Shapley RM (1982), *X and Y cells in the lateral geniculate nucleus of macaque monkeys*. J Physiol, **330**: p. 125–43.
102. Kaplan E, Shapley RM (1986), *The primate retina contains two types of ganglion cells, with high and low contrast sensitivity*. Proc Natl Acad Sci USA, **83**(8): p. 2755–7.
103. Knierim JJ, van Essen DC (1992), *Neuronal responses to static texture patterns in area V1 of the alert macaque monkey*. J Neurophysiol, **67**(4): p. 961–80.
104. Kolb H, Dekorver L (1991), *Midget ganglion cells of the parafovea of the human retina: a study by electron microscopy and serial section reconstructions*. J Comp Neurol, **303**(4): p. 617–36.
105. Kolb H, Linberg KA, Fisher SK (1992), *Neurons of the human retina: a Golgi study*. J Comp Neurol, **318**(2): p. 147–87.
106. Kolb H, Marshak D (2003), *The midget pathways of the primate retina*. Doc Ophthalmol, **106**(1): p. 67–81.
107. Lachica EA, Beck PD, Casagrande VA (1992), *Parallel pathways in macaque monkey striate cortex: anatomically defined columns in layer III*. Proc Natl Acad Sci USA, **89**(8): p. 3566–70.
108. Laubrock J, Engbert R, Kliegl R (2008), *Fixational eye movements predict the perceived direction of ambiguous apparent motion*. J Vis, **8**(14): p. 1–17.
109. Leventhal AG, Rodieck RW, Dreher B (1981), *Retinal ganglion cell classes in the old world monkey: morphology and central projections*. Science, **213**(4512): p. 1139–42.
110. Levitt JB, Lund JS (2002), *The spatial extent over which neurons in macaque striate cortex pool visual signals*. Vis Neurosci, **19**(4): p. 439–52.
111. Livingstone M, Hubel D (1988), *Segregation of form, color, movement, and depth: anatomy, physiology, and perception*. Science, **240**(4853): p. 740–9.
112. Livingstone MS, Hubel DH (1982), *Thalamic inputs to cytochrome oxidase-rich regions in monkey visual cortex*. Proc Natl Acad Sci USA, **79**(19): p. 6098–101.
113. Livingstone MS, Hubel DH (1984), *Anatomy and physiology of a color system in the primate visual cortex*. J Neurosci, **4**(1): p. 309–56.
114. Lorente de Nó R (1949), *Cerebral cortex: architecture, intracortical connections, motor projections*, in *Physiology of the nervous system*, Fulton JF, Editor. Oxford University Press: Oxford. p. 288–330.
115. Lowel S, Schmidt KE, Kim DS, et al. (1998), *The layout of orientation and ocular dominance domains in area 17 of strabismic cats*. Eur J Neurosci, **10**(8): p. 2629–43.
116. Lund JS (1973), *Organization of neurons in the visual cortex, area 17, of the monkey (Macaca mulatta)*. J Comp Neurol, **147**(4): p. 455–96.
117. Lund JS, Boothe RG, Lund RD (1977), *Development of neurons in the visual cortex (area 17) of the monkey (Macaca nemestrina): a Golgi study from fetal day 127 to postnatal maturity*. J Comp Neurol, **176**(2): p. 149–88.
118. Lund JS, Lund RD, Hendrickson AE, et al. (1975), *The origin of efferent pathways from the primary visual cortex, area 17, of the macaque monkey as shown by retrograde transport of horseradish peroxidase*. J Comp Neurol, **164**(3): p. 287–303.
119. Lund JS, Wu CQ (1997), *Local circuit neurons of macaque monkey striate cortex: IV. Neurons of laminae 1–3A*. J Comp Neurol, **384**(1): p. 109–26.
120. Macknik SL (2006), *Visual masking approaches to visual awareness*. Prog Brain Res, **155**: p. 177–215.
121. Macknik SL, Haglund MM (1999), *Optical images of visible and invisible percepts in the primary visual cortex of primates*. Proc Natl Acad Sci USA, **96**(26): p. 15208–10.
122. Macknik SL, Livingstone MS (1998), *Neuronal correlates of visibility and invisibility in the primate visual system*. Nat Neurosci, **1**(2): p. 144–9.
123. Macknik SL, Martinez-Conde S (2004), *The spatial and temporal effects of lateral inhibitory networks and their relevance to the visibility of spatiotemporal edges*. Neurocomputing, **58–60**: p. 775–82.

124. Macknik SL, Martinez-Conde S (2007), *The role of feedback in visual masking and visual processing*. Adv Cogn Psychol, **3**: p. 125–52.
125. Macknik SL, Martinez-Conde S (2009), *The role of feedback in visual attention and awareness*, in *The Cognitive Neurosciences, 4th edition*, Gazzaniga MS, Editor. MIT Press: Cambridge, MA, p. 1165–75.
126. Macknik SL, Martinez-Conde S, Haglund MM (2000), *The role of spatiotemporal edges in visibility and visual masking*. Proc Natl Acad Sci USA, **97**(13): p. 7556–60.
127. Macknik SL, Martinez-Conde S (2009), *Encyclopedia of Perception*, Ed. E. Bruce Goldstein, Sage Press, 522–24.
128. MacNeil MA, Masland RH (1998), *Extreme diversity among amacrine cells: implications for function*. Neuron, **20**(5): p. 971–82.
129. Maguire WM, Baizer JS (1984), *Visuotopic organization of the prelunate gyrus in rhesus monkey*. J Neurosci, **4**(7): p. 1690–704.
130. Malach R, Amir Y, Harel M, Grinvald A (1993), *Relationship between intrinsic connections and functional architecture revealed by optical imaging and in vivo targeted biocytin injections in primate striate cortex*. Proc Natl Acad Sci USA, **90**(22): p. 10469–73.
131. Marks WB, Dobelle WH, Macnichol EF, Jr. (1964), *Visual pigments of single primate cones*. Science, **143**: p. 1181–3.
132. Marr D, Hildreth E (1980), *Theory of edge detection*. Proc R Soc Lond Series B, **207**: p. 187–217.
133. Martinez-Conde S, Cudeiro J, Grieve KL, et al. (1999), *Effects of feedback projections from area 18 layers 2/3 to area 17 layers 2/3 in the cat visual cortex*. J Neurophysiol, **82**(5): p. 2667–75.
134. Martinez-Conde S, Macknik SL (2001). *Junctions are the most salient visual features in the early visual system*, in *Society for Neuroscience 31st Annual Meeting*. San Diego, CA.
135. Martinez-Conde S, Macknik SL (2007), *Windows on the mind*. Sci Am, **297**(2): p. 56–63.
136. Martinez-Conde S, Macknik SL (2008), *Fixational eye movements across vertebrates: comparative dynamics, physiology, and perception*. J Vis, **8**(14): p. 1–16.
137. Martinez-Conde S, Macknik SL, Hubel DH (2000), *Microsaccadic eye movements and firing of single cells in the striate cortex of macaque monkeys*. Nature Neuroscience, **3**(3): p. 251–8.
138. Martinez-Conde S, Macknik SL, Hubel DH (2002), *The function of bursts of spikes during visual fixation in the awake primate lateral geniculate nucleus and primary visual cortex*. Proc Natl Acad Sci USA, **99**(21): p. 13920–5.
139. Martinez-Conde S, Macknik SL, Hubel DH (2004), *The role of fixational eye movements in visual perception*. Nat Rev Neurosci, **5**: p. 229–40.
140. Martinez-Conde S, Macknik SL, Troncoso XG, Dyar TA (2006), *Microsaccades counteract visual fading during fixation*. Neuron, **49**(2): p. 297–305.
141. Martinez-Conde S, Macknik SL, Troncoso XG, Hubel DH (2009), *Microsaccades: a neurophysiological analysis*. Trends Neurosci, **32**(9): p. 463–75.
142. Martinez LM, Alonso JM (2001), *Construction of complex receptive fields in cat primary visual cortex*. Neuron, **32**: p. 515–25.
143. Martinez LM, Wang Q, Reid RC, et al. (2005), *Receptive field structure varies with layer in the primary visual cortex*. Nat Neurosci, **8**(3): p. 372–9.
144. Masland RH, Ames A, 3rd (1976), *Responses to acetylcholine of ganglion cells in an isolated mammalian retina*. J Neurophysiol, **39**(6): p. 1220–35.
145. Maunsell JH, Newsome WT (1987), *Visual processing in monkey extrastriate cortex*. Annu Rev Neurosci, **10**: p. 363–401.
146. McGuire BA, Gilbert CD, Rivlin PK, Wiesel TN (1991), *Targets of horizontal connections in macaque primary visual cortex*. J Comp Neurol, **305**(3): p. 370–92.
147. Meadows JC (1974), *The anatomical basis of prosopagnosia*. J Neurol Neurosurg Psychiatry, **37**(5): p. 489–501.
148. Meadows JC (1974), *Disturbed perception of colours associated with localized cerebral lesions*. Brain, **97**(4): p. 615–32.
149. Merigan WH, Maunsell JH (1993), *How parallel are the primate visual pathways?* Annu Rev Neurosci, **16**: p. 369–402.
150. Miller RF, Slaughter MM (1986), *Excitatory amino acid receptors of the retina: diversity and subtype and conductive mechanisms*. TINS, **9**: p. 211–3.

151. Mishkin M, Ungerleider LG (1983), *Object vision and spatial vision: two cortical pathways*. *Trends Neurosci*, **6**: p. 414–7.
152. Mollon JD, Bowmaker JK (1992), *The spatial arrangement of cones in the primate fovea*. *Nature*, **360**(6405): p. 677–9.
153. Mountcastle VB (1957), *Modality and topographic properties of single neurons of cat's somatic sensory cortex*. *J Neurophysiol*, **20**(4): p. 408–34.
154. Mountcastle VB, Berman AL, Davies PW (1955), *Topographic organization and modality representation in first somatic area of cat's cerebral cortex by method of singleunit analysis*. *Am J Physiol*, **183**: p. 646.
155. Movshon JA, Thompson ID, Tolhurst DJ (1978), *Spatial summation in the receptive fields of simple cells in the cat's striate cortex*. *J Physiol*, **283**: p. 53–77.
156. Muller JF, Dacheux RF (1997), *Alpha ganglion cells of the rabbit retina lose antagonistic surround responses under dark adaptation*. *Vis Neurosci*, **14**(2): p. 395–401.
157. Murphy PC, Duckett SG, Sillito AM (1999), *Feedback connections to the lateral geniculate nucleus and cortical response properties*. *Science*, **286**(5444): p. 1552–4.
158. Murphy PC, Sillito AM (1987), *Corticofugal feedback influences the generation of length tuning in the visual pathway*. *Nature*, **329**(6141): p. 727–9.
159. Nawy S, Copenhagen DR (1987), *Multiple classes of glutamate receptor on depolarizing bipolar cells in retina*. *Nature*, **325**(6099): p. 56–8.
160. Nelson R, Famiglietti EV, Jr., Kolb H (1978), *Intracellular staining reveals different levels of stratification for on- and off-center ganglion cells in cat retina*. *J Neurophysiol*, **41**(2): p. 472–83.
161. Nelson R, Kolb H (1983), *Synaptic patterns and response properties of bipolar and ganglion cells in the cat retina*. *Vision Res*, **23**(10): p. 1183–95.
162. Obermayer K, Blasdel GG (1993), *Geometry of orientation and ocular dominance columns in monkey striate cortex*. *J Neurosci*, **13**(10): p. 4114–29.
163. Olavarria JF, Van Essen DC (1997), *The global pattern of cytochrome oxidase stripes in visual area V2 of the macaque monkey*. *Cereb Cortex*, **7**(5): p. 395–404.
164. Østerberg G (1935), *Topography of the layer of rods and cones in the human retina*. *Acta Ophthalmologica*, **6**: p. 1–103.
165. Pack CC, Livingstone MS, Duffy KR, Born RT (2003), *End-stopping and the aperture problem: two-dimensional motion signals in macaque V1*. *Neuron*, **39**(4): p. 671–80.
166. Pasupathy A, Connor CE (1999), *Responses to contour features in macaque area V4*. *J Neurophysiol*, **82**(5): p. 2490–502.
167. Pearlman AL, Birch J, Meadows JC (1979), *Cerebral color blindness: an acquired defect in hue discrimination*. *Ann Neurol*, **5**(3): p. 253–61.
168. Peichl L, Wässle H (1983), *The structural correlate of the receptive field centre of alpha ganglion cells in the cat retina*. *J Physiol*, **341**: p. 309–24.
169. Perkel DJ, Bullier J, Kennedy H (1986), *Topography of the afferent connectivity of area 17 in the macaque monkey: a double-labelling study*. *J Comp Neurol*, **253**(3): p. 374–402.
170. Perry VH, Cowey A (1981), *The morphological correlates of X- and Y-like retinal ganglion cells in the retina of monkeys*. *Exp Brain Res*, **43**(2): p. 226–8.
171. Perry VH, Oehler R, Cowey A (1984), *Retinal ganglion cells that project to the dorsal lateral geniculate nucleus in the macaque monkey*. *Neuroscience*, **12**(4): p. 1101–23.
172. Poggio GF, Doty RW, Jr., Talbot WH (1977), *Foveal striate cortex of behaving monkey: single-neuron responses to square-wave gratings during fixation of gaze*. *J Neurophysiol*, **40**(6): p. 1369–91.
173. Polyak S (1941), *The retina*. Chicago: University of Chicago Press.
174. Powell TP, Mountcastle VB (1959), *Some aspects of the functional organization of the cortex of the postcentral gyrus of the monkey: a correlation of findings obtained in a singleunit analysis with cytoarchitecture*. *Bull Johns Hopkins Hosp*, **105**: p. 133–62.
175. Ramón y Cajal S (1893), *La rétine des vertébrés*. *Cellule*, **9**: p. 117–257.
176. Ramón y Cajal S (1900), *Structure of the Mammalian Retina*. Madrid.

177. Rao RPN, Olshausen BA, Lewicki MS (2002), *Probabilistic models of the brain: perception and neural function*. Cambridge, MA: MIT Press.
178. Ratcliff G, Davies-Jones GA (1972), *Defective visual localization in focal brain wounds*. *Brain*, **95**(1): p. 49–60.
179. Ratliff F (1965), *Mach bands: Quantitative studies on neural networks in the retina*. San Francisco: Holden-Day, Inc.
180. Reid RC, Alonso JM (1995), *Specificity of monosynaptic connections from thalamus to visual cortex*. *Nature*, **378**(6554): p. 281–4.
181. Ringach DL (2002), *Orientation selectivity in macaque V1: diversity and laminar dependence*. *J Neurosci*, **22**(13): p. 5639–51.
182. Ringach DL (2002), *Spatial structure and symmetry of simple cell receptive fields in macaque primary visual cortex*. *J Neurophysiol*, **88**: p. 455–463.
183. Rockland KS, Lund JS (1983), *Intrinsic laminar lattice connections in primate visual cortex*. *J Comp Neurol*, **216**(3): p. 303–18.
184. Rockland KS, Saleem KS, Tanaka K (1994), *Divergent feedback connections from areas V4 and TEO in the macaque*. *Vis Neurosci*, **11**(3): p. 579–600.
185. Rockland KS, Virga A (1989), *Terminal arbors of individual “feedback” axons projecting from area V2 to V1 in the macaque monkey: a study using immunohistochemistry of anterogradely transported Phaseolus vulgaris-leucoagglutinin*. *J Comp Neurol*, **285**(1): p. 54–72.
186. Rodieck RW (1998), *The first steps in seeing*. Sunderland, Massachusetts: Sinauer Associates. 562.
187. Roorda A, Williams DR (1999), *The arrangement of the three cone classes in the living human eye*. *Nature*, **397**(6719): p. 520–2.
188. Sceniak MP, Hawken MJ, Shapley R (2001), *Visual spatial characterization of macaque V1 neurons*. *J Neurophysiol*, **85**(5): p. 1873–87.
189. Schiller PH, Malpel JG (1978), *Functional specificity of lateral geniculate nucleus laminae of the rhesus monkey*. *J Neurophysiol*, **41**(3): p. 788–97.
190. Schultze M (1866), *Zur Anatomie und Physiologie der Retina*. *Arch Mikrosk Anat Entwicklungsmech*, **2**: p. 165–286.
191. Shapley R, Hawken M, Ringach DL (2003), *Dynamics of orientation selectivity in the primary visual cortex and the importance of cortical inhibition*. *Neuron*, **38**(5): p. 689–99.
192. Shapley R, Perry JS (1986), *Cat and monkey retinal ganglion cells and their visual functional roles*. *Trends Neurosci*, **9**: p. 229–35.
193. Sherman SM, Guillery RW (1998), *On the actions that one nerve cell can have on another: distinguishing “drivers” from “modulators”*. *Proc Natl Acad Sci USA*, **95**(12): p. 7121–6.
194. Sherman SM, Guillery RW (2001), *Exploring the thalamus*. San Diego: Academic Press.
195. Shipp S, Zeki S (1985), *Segregation of pathways leading from area V2 to areas V4 and V5 of macaque monkey visual cortex*. *Nature*, **315**(6017): p. 322–5.
196. Shipp S, Zeki S (1989), *The organization of connections between areas V5 and V1 in macaque monkey visual cortex*. *Eur J Neurosci*, **1**(4): p. 309–32.
197. Sincich LC, Horton JC (2005), *The circuitry of V1 and V2: integration of color, form, and motion*. *Annu Rev Neurosci*, **28**: p. 303–26.
198. Skavenski AA, Hansen RM, Steinman RM, Winterson BJ (1979), *Quality of retinal image stabilization during small natural and artificial body rotations in man*. *Vision Res*, **19**(6): p. 675–83.
199. Slaughter MM, Miller RF (1981), *2-amino-4-phosphonobutyric acid: a new pharmacological tool for retina research*. *Science*, **211**(4478): p. 182–5.
200. Slaughter MM, Miller RF (1983), *An excitatory amino acid antagonist blocks cone input to sign-conserving second-order retinal neurons*. *Science*, **219**(4589): p. 1230–2.
201. Steriade M, Jones EG, McCormick DA, eds (1997). *Thalamus*. Elsevier: New York.
202. Stone J, Dreher B, Leventhal A (1979), *Hierarchical and parallel mechanisms in the organization of visual cortex*. *Brain Res*, **180**(3): p. 345–94.
203. Suzuki W, Saleem KS, Tanaka K (2000), *Divergent backward projections from the anterior part of the inferotemporal cortex (area TE) in the macaque*. *J Comp Neurol*, **422**(2): p. 206–28.

204. Tomita T (1965), *Electrophysiological study of the mechanisms subserving color coding in the fish retina*. Cold Spring Harb Symp Quant Biol, **30**: p. 559–66.
205. Trifonov YA (1968), *Study of synaptic transmission between the photoreceptor and the horizontal cell using electrical stimulation of the retina*. Biofizika, **10**: p. 673–80.
206. Troncoso XG, Macknik SL, Martinez-Conde S (2005), *Novel visual illusions related to Vasarely's 'nested squares' show that corner salience varies with corner angle*. Perception, **34**(4): p. 409–20.
207. Troncoso XG, Macknik SL, Martinez-Conde S (2008), *Microsaccades counteract perceptual filling-in*. J Vis, **8**(14): p. 1–9.
208. Troncoso XG, Macknik SL, Martinez-Conde S (2009), *Corner salience varies linearly with corner angle during flicker-augmented contrast: a general principle of corner perception based on Vasarely's artworks*. Spat Vis, **22**(3): p. 211–24.
209. Troncoso XG, Macknik SL, Otero-Millan J, Martinez-Conde S (2008), *Microsaccades drive illusory motion in the Enigma illusion*. Proc Natl Acad Sci USA, **105**(41): p. 16033–8.
210. Troncoso XG, Tse PU, Macknik SL, et al. (2007), *BOLD activation varies parametrically with corner angle throughout human retinotopic cortex*. Perception, **36**(6): p. 808–20.
211. Ts'o DY, Frostig RD, Lieke EE, Grinvald A (1990), *Functional organization of primate visual cortex revealed by high resolution optical imaging*. Science, **249**(4967): p. 417–20.
212. Ts'o DY, Gilbert CD, Wiesel TN (1986), *Relationships between horizontal interactions and functional architecture in cat striate cortex as revealed by cross-correlation analysis*. J Neurosci, **6**(4): p. 1160–70.
213. Ungerleider LG, Desimone R (1986), *Cortical connections of visual area MT in the macaque*. J Comp Neurol, **248**(2): p. 190–222.
214. Ungerleider LG, Desimone R (1986), *Projections to the superior temporal sulcus from the central and peripheral field representations of V1 and V2*. J Comp Neurol, **248**(2): p. 147–63.
215. Ungerleider LG, Mishkin M (1982), *Two cortical visual systems, in Analysis of visual behavior*, Ingle DG, Goodale MA, Mansfield JQ, Editors. MIT Press: Cambridge, MA. p. 549–86.
216. Usrey WM, Alonso JM, Reid RC (2000), *Synaptic interactions between thalamic inputs to simple cells in cat visual cortex*. J Neurosci, **20**(14): p. 5461–7.
217. vanDam LC, van Ee R (2006), *Retinal image shifts, but not eye movements per se, cause alternations in awareness during binocular rivalry*. J Vis, **6**(11): p. 1172–9.
218. Van Essen DC, Anderson CH, Felleman DJ (1992), *Information processing in the primate visual system: an integrated systems perspective*. Science, **255**(5043): p. 419–23.
219. Van Essen DC, Gallant JL (1994), *Neural mechanisms of form and motion processing in the primate visual system*. Neuron, **13**(1): p. 1–10.
220. Van Essen DC, Zeki SM (1978), *The topographic organization of rhesus monkey prestriate cortex*. J Physiol, **277**: p. 193–226.
221. Vasarely V (1970), *Vasarely II*. Plastic arts of the 20th century, ed. Joray M. Switzerland: Éditions du Griffon Neuchâtel.
222. Verweij J, Dacey DM, Peterson BB, Buck SL (1999), *Sensitivity and dynamics of rod signals in H1 horizontal cells of the macaque monkey retina*. Vision Res, **39**(22): p. 3662–72.
223. Wässle H, Boycott BB (1991), *Functional architecture of the mammalian retina*. Physiol Rev, **71**(2): p. 447–80.
224. Watanabe M, Rodieck RW (1989), *Parasol and midget ganglion cells of the primate retina*. J Comp Neurol, **289**(3): p. 434–54.
225. Werblin FS, Dowling JE (1969), *Organization of the retina of the mudpuppy, Necturus maculosus. II. Intracellular recording*. J Neurophysiol, **32**(3): p. 339–55.
226. Wiesel TN, Hubel DH, Lam DM (1974), *Autoradiographic demonstration of ocular-dominance columns in the monkey striate cortex by means of transneuronal transport*. Brain Res, **79**(2): p. 273–9.
227. Wiser AK, Callaway EM (1996), *Contributions of individual layer 6 pyramidal neurons to local circuitry in macaque primary visual cortex*. J Neurosci, **16**(8): p. 2724–39.
228. Yarbus AL (1967), *Eye movements and vision*. New York: Plenum Press.

229. Zeki SM (1974), *Cells responding to changing image size and disparity in the cortex of the rhesus monkey*. J Physiol, **242**(3): p. 827–41.
230. Zeki SM (1974), *Functional organization of a visual area in the posterior bank of the superior temporal sulcus of the rhesus monkey*. J Physiol, **236**(3): p. 549–73.
231. Zeki SM (1978), *Functional specialisation in the visual cortex of the rhesus monkey*. Nature, **274**(5670): p. 423–8.
232. Zeki SM (1978), *Uniformity and diversity of structure and function in rhesus monkey prestriate visual cortex*. J Physiol, **277**: p. 273–90.
233. Zhaoping L (2005), *The primary visual cortex creates a bottom-up saliency map*, in *Neurobiology of Attention*, Itti L, Rees G, Tsotsos JK, Editors. Elsevier: Oxford. p. 570–75.
234. Zihl J, von Cramon D, Mai N (1983), *Selective disturbance of movement vision after bilateral brain damage*. Brain, **106** (Pt2): p. 313–40.

Visual Prosthetics

Physiology, Bioengineering, Rehabilitation

Dagnelie, G. (Ed.)

2011, XVIII, 453 p., Hardcover

ISBN: 978-1-4419-0753-0